Molecular Interactions between Simple Sugars and Styrene Derivatives: Identifying Favorable Binding Agents for Bifunctional Solid Acid Catalysts

Major Qualifying Project Report completed
In partial fulfillment of the requirements for the Degree of Bachelor of Science
At *Worcester Polytechnic Institute*, Worcester, MA

By:
Zachary Burgess
Luke Habib

Advisors:
N. Aaron Deskins
Michael Timko

With Special Assistance from:
Avery Brown
Maksim Tyufekchiev

4/27/2017

Table of Contents

Abstract

The goal of this project was to research the potential for different functional groups as binding domains on solid acid catalysts. Computational analysis was conducted to simulate binding interactions between and calculate adsorption energies for two different functional groups and the stereoisomers of ringed glucose. Experimental analysis was conducted to observe glucose and cellobiose adsorption onto hydroxymethyl styrene polymer beads. Further research needs to be conducted to prove these interactions happen near glycosidic bonds, which is favorable for biofuel production.

Acknowledgements

We would like to begin by thanking our advisors, Professor Michael Timko and Professor Aaron Deskins of the Department of Chemical Engineering at Worcester Polytechnic Institute, for the opportunity to complete this project and their guidance throughout it. They provided constant support and insight as the project progressed while also providing us with the freedom and responsibility to guide this project as we saw fit.

In addition, we'd like to thank PhD candidates Maksim Tyufekchiev and Avery Brown for their intellectual guidance and moral support. Their previous research, laboratory expertise, and computational techniques were vital contributions to developing the scope of our project and executing our methodology. The project would have been much more challenging if it were not for their assistance.

Lastly, we'd like to thank the National Science Foundation for helping to fund parts of our project in accordance with Grant #1554283 which was awarded to Professor Timko.

Chapter 1: Introduction

As evidence mounts about the many anthropogenic causes for climate change, the search for viable alternative energy sources is becoming increasingly critical. Energy stability is of paramount importance to this issue, particularly for countries that rely primarily on foreign sources of energy. Other relevant aspects of this issue are sustainability and environmental impact, as the lack of sustainability and ignorance of impact have catalyzed the current crisis. This is especially important to consider in terms of transportation fuels, which are currently primarily derived from petroleum and account for a large percentage of global energy usage.[1] Because there are few places where petroleum is produced[2] for the rest of the world to consume, and because petroleum, its production and generation, and the products derived from it have generally negative impacts on the environment, diversifying the precursor for transportation fuels and other petroleum based chemicals is a key goal for sustainability and environmentalism.

Biomass has been identified as a promising source of energy, particular as a promising precursor to alternative and sustainable transportation fuels. More specifically, lignocellulosic biomass, which is the source for second generation biofuels, has been identified as a favorable biomass source for a number of reasons, but most notably is more favorable than first generation biofuel sources because the energy crops for lignocellulosic biomass do not compete with food crops.[1] The process to develop biofuels from biomass has three main parts: pretreatment; hydrolysis to

[1] Escobar, J. C., Lora, E. S., Venturini, O. J., Yanez, E. E., Castillo, E. F., & Almazan, O. (2009). Biofuels: Environment, technology and food security. *Renewable and Sustainable Energy Reviews, 13*, 1275-1287. doi:10.1016/j.rser.2008.08.014

[2] Doman, L. (2016, May 23). U.S. Energy Information Administration - EIA - Independent Statistics and Analysis. Retrieved April 23, 2017, from https://www.eia.gov/todayinenergy/detail.php?id=26352

simpler, soluble, and fermentable sugars; and fermentation.[3] This project primarily focuses on the hydrolysis aspect of the process, but also discusses pretreatment. There are a number of pretreatment methods that have been explored in literature, which are used when enzymatic hydrolysis is being used to break the cellulose down.[3] However, the main method explored in this project is hydrolysis by solid acid catalysis, which is typically with a physiochemical pretreatment like ball-milling. Solid acid catalysis has been determined to be more environmentally friendly, sustainable, and less energy intensive than many of the other methods explored in literature.[4,5,6] One of the biggest hurdles that must be overcome to make solid acid catalysis a process that can commercialize biofuel production is to increase the favorability of the interaction between cellulose and the catalyst of choice. Because cellulose is such a large molecule and can be different based on the biomass source, it is important to produce research into the interactions and how to ensure optimal hydrolysis with the desired catalyst. Therein lies the focus of this project.

In this project, the interactions that glucose and cellobiose have with two functional groups, chloromethyl and hydroxymethyl, were studied. This interaction is key to the further development of biofuel production and the use of solid acid catalysts in that process. Currently there is little empirical evidence characterizing the relationship between cellulose, as well as

[3] Xu, Z., & Huang, F. (2014). Pretreatment Methods for Bioethanol Production. *Applied Biochemistry and Biotechnology, 174*, 43-62. doi:10.1007/s12010-014-1015-y

[4] Guo, F., Fang, Z., Xu, C. C., & Smith, R. L. (2012). Solid acid mediated hydrolysis of biomass for producing biofuels. *Progress in Energy and Combustion Science, 38*(5), 672-690. doi:10.1016/j.pecs.2012.04.001

[5] Gupta, P., & Paul, S. (2014). Solid acids: Green alternatives for acid catalysis. *Catalysis Today, 236*, 153-170. doi:10.1016/j.cattod.2014.04.010

[6] Huang, Y., & Fu, Y. (2013). Hydrolysis of cellulose to glucose by solid acid catalysts. *Green Chemistry,* (5), 1095-1111. Retrieved from http://pubs.rsc.org/en/Content/ArticleLanding/2013/GC/c3gc40136g#!divAbstract

simpler sugars, and and these types of catalysts, which has left a hole in the research surrounding this topic. Further, the analyses available are based mainly on the assumption that chloromethyl groups are the more favorable binding agent due to hydrogen bonding,[6] but hydroxymethyl groups should theoretically allow for more hydrogen bonding. Regardless, all conclusions made in the literature about these interactions have been hypothetical and not conclusive. Thus, the analysis conducted in this project was meant to begin this exploration.

This analysis was conducted computationally and experimentally. The computational analysis was conducted using a web-based software to observe modeled interactions between glucose and cellobiose and styrene monomers with a hydroxymethyl functional group attached as well as styrene with a chloromethyl functional group attached. The experimental analysis was conducted with adsorption experiments using glucose and cellobiose solutions at varying concentrations and hydroxymethyl styrene polymer beads. These functional groups were selected as potential binding agents for solid acid catalysts based on available literature. The objective of this project was to determine the more favorable binding agent, which would in turn maximize the hydrolysis pretreatment process.

The following sections of this report will cover more background literature that informed the experiments that were run, the methodology employed, the results of computational analysis and the experiments run, and conclusions as well as suggestions for future work based on the results collected. The following background section will go further in depth into the need for alternative

energy sources, the structure of cellulose, different pretreatment methods explored in literature, and the favorability of solid acid catalysis as a hydrolysis pretreatment method.

Chapter 2: Background

There is increasing demand for alternative, environmentally friendly, and sustainable energy sources for number of reasons.[1,7,8,9] There has been increased awareness and higher levels of activism around the world demonstrating that need and the desire of a large portion of the world's population to employ more sustainable practices across the board. People are realizing and accepting more and more the anthropogenic causes of climate change as well as the tangible, adverse effects that climate change will have in our lifetimes, regardless of its causes. Climate change poses an imminent threat to a number of species on Earth, including humans who have seen over 100,000 deaths per year because of its effects.[1] It is well known and understood that the availability of fossil fuels are not endless. It is not easy to know exactly how much is left, because new sources are discovered with moderate frequency; however, as countries continue to develop and the human population continues to grow, energy demand will continue to rise and fossil fuels take millions of years to develop.[1] Figure 1 below shows the current proven oil reserves in the world. There is no question that the sources will run out, the question is when and the problem with not knowing when is that it is likely that no one will know until it is too late.[1] It is for these major reasons that the call for a robust and competitive alternative energy market emerge in the near future.

---

[7] Field, C., Campbell, J., & Lobell, D. (2008). Biomass energy: the scale of the potential resource. *Trends in Ecology & Evolution, 23*(2), 65-72. doi:10.1016/j.tree.2007.12.001

[8] Hoogwijk, M., Faaij, A., Broek, R. V., Berndes, G., Gielen, D., & Turkenburg, W. (2003). Exploration of the ranges of the global potential of biomass for energy. *Biomass and Bioenergy, 25*(2), 119-133. doi:10.1016/s0961-9534(02)00191-5

[9] Berndes, G., Hoogwijk, M., & van den Broek, R. (2003). The contribution of biomass in the future global energy supply: a review of 17 studies. *Biomass and bioenergy*, *25*(1), 1-28. doi: 10.1016/S0961-9534(02)00185-X

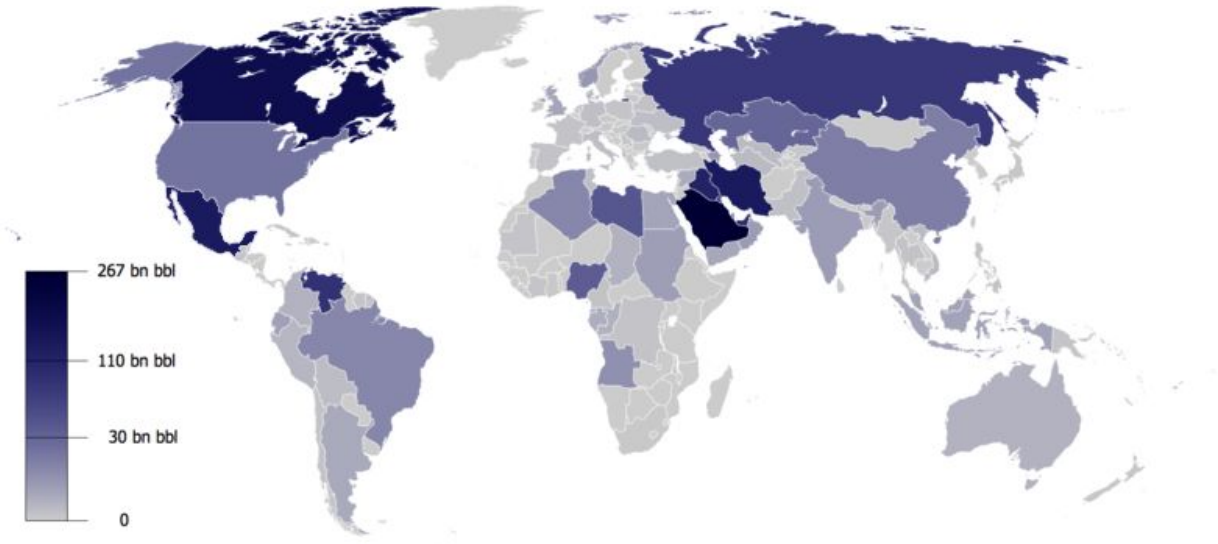

Figure 1: Current proven oil reserves in the world in billions of barrels of oil - as of 2014

In this project, cellulose source and pretreatment methods are specifically laid out and will be discussed further in depth in the coming sections. The biomass of interest here is lignocellulosic biomass, often referred to as a second generation biofuel source. The pretreatment method of interest is hydrolysis catalyzed by solid acids. Lignocellulosic biomass is abundantly available and is not cellulose typically derived from food crops, but rather the biomass left behind from food crops in the form of agricultural residues as well as other sources such as wood and grass.[3] These biomass sources can also develop a number of different kinds of fuels like ethanol, butanol, hydrogen, and methane, as well as the other chemicals described above.[3] Solid acid catalysis is a more recent development in the search for an appropriate pretreatment method for breaking cellulose chains down into soluble sugars like glucose. Solid acids are generally easier to separate from the products, therefore making them easier to recycle making them more sustainable catalysts.[4,5,6] Though there are complications associated with both of those specifications, they have prevailed as the ideal source and method, respectively, within the field

of biofuel production. Before getting into the specifics of how solid acid catalysts hydrolyze cellulose and why solid acid catalysis was studied in this project, it is valuable to spend some time discussing more general background topics, as well as more specific background surround cellulose and the different available solid acid catalysts.

2.1 Biomass as a Source of Transportation Fuel

A number of alternative energy technologies have gained traction, such as solar and wind power, but these are popular mainly for personal and industrial use on a power grid. The issue of replacing petroleum gasoline as the energy source for transportation is complicated, but biomass has proven to be one of the most promising sources of renewable liquid fuel for transportation purposes.[1,3,6,7,8,9,10] Biomass energy is one of the oldest sources of energy and still used today in the form of wood burning, for instance. More recently, scientists have been able to identify ways to reduce biomass to soluble sugars and further processed into a number of fuels. Biofuels, primarily in the form of bio-ethanol and biodiesel, are relatively frequently used now as fuels or fuel additives.[7] This current market and use for biofuels provide a solid foundation for the expansion of their market production, particularly because infrastructure already exists. This existing infrastructure is one of the most notable advantages of biofuels over electric powered cars since implementation of biofuels would be less likely to disrupt current consumption and could be implemented quickly. Further, biofuels are being produced so that they can be used seamlessly in internal combustion engines that are already used in cars and trucks.

[10] Butera, G., De Pasquale, C., Maccotta, A., Alonzo, G., & Conte, P. (2011). Thermal transformation of micro-crystalline cellulose in phosphoric acid. *Cellulose*, *18*(6), 1499-1507. doi: 10.1007/s10570-011-9590-3

Besides the practicality of looking to biomass for a renewable alternative source of fuel, it passes the sustainability test as well. While biofuels still emit similarly to petroleum based fuels, theoretically all of the CO_2 is used by future energy crops effectively making biofuels net-zero CO_2 emitters. Since biomass comes from plants and algae, it is considered renewable so long as the species being used do not go extinct. Further, biofuels can be developed from a number of different biomass sources.[1,7,8,9,10] The type of biomass used for fuel can be adapted to the available resources of the surrounding area. Since biofuels are more able to be locally sourced, energy insecurity can be mediated in places where there are not other sources readily available and countries without oil resources can be less dependent on foreign oil imports. Beyond fuels, many chemicals in wide use today are derived from petroleum. These chemicals can be replaced by chemicals derived from biomass, and these are often termed green chemicals. The chemicals include acetic acid, malic acid, acetone, lactic acid, and more.[1] Biofuels and green chemicals can be processed in the same sites, often called biorefineries. Another important advantage to biomass is that it can be grown on degraded land than is needed for food crops, meaning that it does not need to compete with food crops for space. Further, over time it can improve the land if it is continuously grown there. This avoids a potential hurdle to biomass as a viable source of energy, because between energy needs and food needs, societies will typically prioritize land for food.[1] There are, however, a number of other hurdles that need to be considered.

The first major hurdle that must be addressed is that many believe there are insufficient means for biomass to fully replace petroleum based fuels.[7] This does not necessarily disqualify biomass as a viable option for future liquid transportation fuels, but it does mean that other major sources

of energy need to be explored as well as potential smaller supplements. The concept of consumption is also important to discuss as it pertains to sustainability and environmentalism. It's not enough to just replace energy from fossil fuels to that from renewable clean technologies, society has to make strides towards energy efficiency in technology and practice to ease the transition.[1,7]

There are other environmentally-related concerns when it comes to biofuel production. As mentioned before, there is the idea of competition of crops and land with the food crop industry. This is essentially a non starter in most cases, with the preference towards food over energy.[1,7] When that is not the issue at hand, there is also the possibility that forested land would be razed for energy crop farming. This is problematic because forests are carbon sinks so realistically this would result in higher overall carbon emissions. There is also the potential for pollution at all levels of production, starting with chemicals used for agricultural purposes.[7] Other than that, some of the proposed methods for converting biomass to biofuels use strong acids that can be corrosive and difficult to separate and recycle, some methods are very energy intensive, some have very low yields of soluble sugars, and so on.[1,7,8,9,10] Within the realm of environmental impact and sustainability, there are a lot of variables to optimize to ensure that the use of biomass is truly a positive shift. Land choice, agricultural techniques, processing methods, and even cellulose source all need to be considered.

2.2 Lignocellulosic Biomass

Lignocellulosic biomass is the ideal biomass source for biofuel production and solid acid mediated catalysis is the best option for hydrolysis. Lignocellulosic biomass is abundantly available from a variety of sources including wood, grass, and agricultural and forest residues. This makes it widely available, as mentioned before, and generally accessible in many locations that may be otherwise dependent on foreign sources of oil. This form of cellulose also does not compete with food because it typically comes from inedible portions of plants and agricultural residues such as corn stalks as opposed to the corn itself. A variety of fuels can be derived from lignocellulosic biomass such as ethanol, butanol, hydrogen, and methane, as well as a number of green chemicals as mentioned above.[3] Solid acid catalysis is much more environmentally friendly and sustainable than other hydrolysis methods. The most notable differences between solid acid catalysis and liquid acid catalysis are the lower risk of corrosion to reactors and the relative ease of extracting the solid acids at the end of the process.[4,5,6] To fully understand why these two parameters were chosen for further study in this project, they must be more thoroughly discussed, starting with the structure of cellulose and how that dictates the process for deriving fuels from these sources.

2.3 Structure of Cellulose

Cellulose is the most abundant polymer on earth. It is one of the main constituents of plants where its primary role is to help maintain the structure. In plants, cellulose is typically found in any of the woody portions of plant tissues, such as the stem or stalk of the plant. It is present in fungi, algae, and even some animals. As far as structure, in short cellulose is a fibrous, tough,

water insoluble, unbranched homopolysaccharide. It is comprised of beta-D-glucopyranose units linked by (1→4) glycosidic bonds and has a degree of polymerization between 1,000 and 15,000 depending on the source of cellulose.[11] An example of a cellulose structure with hydrogen bonding can be seen below in Figure 2.

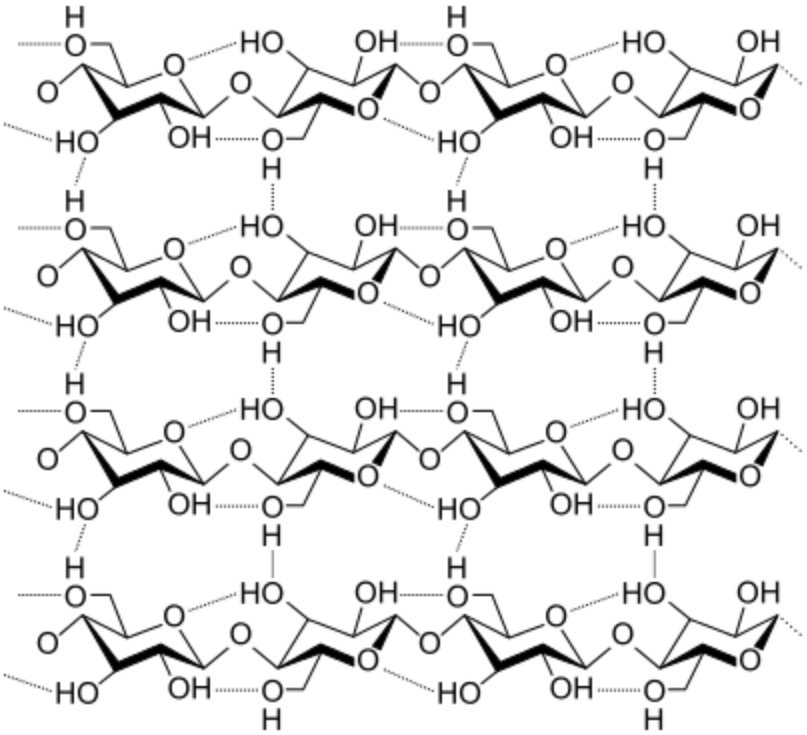

Figure 2: Four strands of cellulose, dotted lines representing the intricate hydrogen bonding within the strands

There are seven polymorphs of cellulose known as I_{alpha}, I_{beta}, II, III_{I}, III_{II}, IV_{I}, and IV_{II}. However, the polymorphs of cellulose typically found in nature are I_{alpha} and I_{beta} and this form of cellulose is also known as native cellulose. Though the cellulose I polymorphs are the forms found in nature, it is not the most thermodynamically stable form, that is actually cellulose II, but the formation of cellulose in nature yields cellulose 1 polymorphs because of the proteins typically

[11] O'sullivan, A. C. (1997). Cellulose: the structure slowly unravels. *Cellulose*, *4*(3), 173-207.

involved in that process. Further, between I_{alpha} and I_{beta}, I_{beta} is more stable. These two polymorphs are very similar except for their hydrogen bonding patterns. Most cellulose samples in nature contain both polymorphs, with differing ratios depending on the source, and no sources have been found with pure I_{alpha} because it is only a metastable polymorph. The discovery of the two polymorphs of cellulose I was made once scientists discovered that there were different forms of cellulose at the surface of a cellulose crystal and at the center. Because I_{alpha} is metastable, the proportion of I_{alpha} and I_{beta} can affect the reactivity of the native cellulose source. This proportion is highest in bacterial cellulose sources. Cellulose I_{alpha} can be converted to I_{beta} by annealing at approximately 270 ^{o}C.[11]

Crystallinity and the presence of lignin are the main aspects of the structure of cellulose that call for pretreatment. Cellulose and hemicellulose are tightly packed in cellulose sources by lignin, which serves to protect plants and other sources of cellulose from chemical alterations, notably enzymatic hydrolysis which is the among most popular methods for converting cellulose to fermentable sugars. High crystallinity restricts these kinds of processes as well. Cellulose has crystalline and amorphous sites throughout its crystals, and even along one microfibril.[11] The amorphous sites are those of interest because they are easier to hydrolyze, so the purpose of cellulose pretreatment is to break down the crystalline sites to make the amorphous sites more accessible for enzymatic hydrolysis.[12] The many different methods for hydrolysis and pretreatment are explained below, as well as why solid acid catalysis is the preferred method and the method we focused on in this project.

[12] Zhao, H., Kwak, J. H., Wang, Y., Franz, J. A., White, J. M., & Holladay, J. E. (2006). Effects of Crystallinity on Dilute Acid Hydrolysis of Cellulose by Cellulose Ball-Milling Study. *Energy & Fuels, 20*(2), 807-811. doi:10.1021/ef050319a

2.4 History and Production of Biofuels

In the search for sustainable and clean energy sources, the world has developed three generations of biofuels. The first generation are produced directly from food crops.[13] The second generation is similar to the first in the sense that it comes from a feedstock of plants, but the second generation does not use food crops.[14] The third and most recent generation consists of biofuels derived from algae.[15] All three generations are capable of producing bioethanol with the same chemical structure. For the purpose of this paper, the second generation was primarily researched because most of its feedstock consists of the lignocellulose component that is considered in the background research focused on the interactions of the solid acid catalyst. Figure 3 shows an overview of the process for breaking down lignocellulose and converting it into fuels and other chemicals.

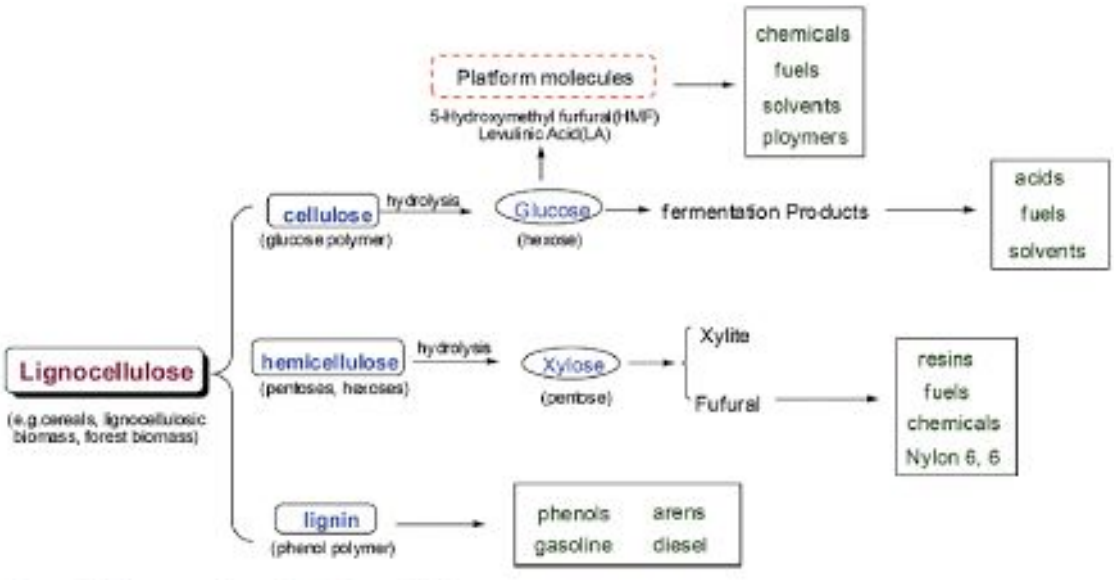

Figure 3: Utilization of lignocelluloses to produce chemicals and fuels.[14]

[13] First Generation Biofuels. (n.d.). Retrieved from http://biofuel.org.uk/first-generation-biofuel.html
[14] Second Generation Biofuels. (n.d.). Retrieved from http://biofuel.org.uk/second-generation-biofuels.html
[15] Third Generation Biofuels. (n.d.). Retrieved from http://biofuel.org.uk/third-generation-biofuels.html

For the biomass gathered to begin the transformation into bioethanol it first needs to be broken down so that the cellulose within the biomass can be converted into fermentable sugars.[3] Lignocellulosic biomass consists of a densely packed structure of cellulose, hemicellulose, and lignin.[3] Hemicellulose is a heteropolymer, a polymer composed of more than one kind of monomer, of pentoses, hexoses, and sugar acids.[16,17] Lignin is a complex organic polymer which serves multiple functions within a plant, most significantly how it protects the plant from enzymatic hydrolysis.[3] The main objective of pretreatment is to disrupt the recalcitrance effect of the lignin to make the cellulose accessible for hydrolysis.[3] To start, the biomass is almost always milled up into smaller components to release starch components.[18] The milled up feedstock can then undergo a number of pretreatment methods: acidic pretreatment, neutral pretreatment, alkaline pretreatment, and ozonolysis.[3] Each of which uses a different solution to help disrupt the lignin. Moreover, these different pretreatment methods can be classified by the primary mechanism that acts on the lignocellulosic biomass during pretreatment: physical, physicochemical, and chemical pretreatments. Pretreatment methods vary depending on what the biomass feedstock is and which hydrolysis method it will undergo.

[16] Murthy, G. S. (n.d.). *Cellulose, Hemicellulose and Lignin*. Lecture presented at Lecture Six in Oregon State University, Corvallis, OR. Retrieved from http://stl.bee.oregonstate.edu/courses/BFP/Class_Slides_W2011/BFP_Lecture6.pdf
[17] Blamire, J. (1999). The Giant Molecules of Life: Monomers and Polymers. Retrieved from http://www.brooklyn.cuny.edu/bc/ahp/SDPS/SD.PS.polymers.html
[18] Bioethanol: Production Processes. (n.d.). Retrieved from http://www.cropenergies.com/en/Bioethanol/Produktionsverfahren/

After the biomass solution has been pretreated, it undergoes a conversion from ligno-cellulose into sugar through enzymatic hydrolysis.[19] Essentially, this is the stage of bioethanol production where cellulose is broken down into glucose and hemicellulose is broken down into xylose.[6] The established methods for hydrolysis rely on the use of cellulose enzymes, also known as cellulases.[11] The use of these enzymes is limited though as the hydrolysis process is not very efficient and the enzymes are expensive.[11] Efforts have been made to increase the effectiveness of cellulases by increasing the amount introduced to the system, but this only increases the already high cost.[20] In addition, liquid acid catalysts have been used for the hydrolysis of cellulose since the early 19th century.[11] Despite being more efficient than cellulases, the use of liquid acid catalysts also has negative consequences. Liquid acid systems have major problems with product/catalyst separation, reactor corrosion, catalyst recycling, and waste treatment.[11] As a result, solid acid catalysts are being explored as possible replacements for cellulases and liquid acids. More information on the use of solid acid catalysts for glucose hydrolysis is discussed in the following section, Section 2.5**.**

Following the conversion of cellulose into glucose, the glucose solution undergoes fermentation and is converted to ethanol. Fermentation is a biological process in which microorganisms such as bacteria, yeasts, and fungi metabolize sugars into acids, gases, or alcohol. Yeast is the most commonly used microorganism and it produces ethanol and carbon dioxide from the glucose

[19] Biofuel Production. (2007). *IEA Energy Technology Essentials,* 1-4. Retrieved from https://www.iea.org/publications/freepublications/publication/essentials2.pdf.
[20] Sun, Y., & Cheng, J. (2002). Hydrolysis of lignocellulosic materials for ethanol production: a review. *Bioresource Technology,83*(1), 1-11. Retrieved from http://www.sciencedirect.com/science/article/pii/S0960852401002127

solution. Depending on the yeast chosen and the initial concentration of glucose, almost 50 g/L of ethanol can be produced.[21]

Once the ethanol has been produced from fermentation, it must be separated from the rest of the solution through distillation. Through distillation, most of the water is removed from the solution. A low level of water remains to prevent the formation of a low-boiling water-ethanol azeotrope.[22]

2.5 Solid Acid Catalysis

Solid acid catalysts are being researched more and more as a potential mechanism for the hydrolysis of cellulose and hemicellulose in bioethanol production because of their potential upside over enzymatic or dilute acid hydrolysis. Solid acid catalysts are favored over dilute liquid acids because they easier to separate from the product, recycle, and cause less damage to the reactor vessel.[11] They also produce higher yields of glucose when compared to enzymatic hydrolysis.[11] SAC's are typically described for their Brønsted/Lewis sites, the strength and number of these sites, and the surface area and porosity of their support base.[11] In this section we will review the different types of solid acid catalysts and the progress being made, but specifically focus on polymer based solid acid catalysts.

[21] Lin, Y., & Tanaka, S. (2006). Ethanol fermentation from biomass resources: current state and prospects. *Applied Microbiology and Biotechnology,69*(6), 627-642. Retrieved from https://link.springer.com/article/10.1007/s00253-005-0229-x.
[22] Bioethanol Production. (n.d.). Retrieved from http://www.makebiofuel.co.uk/bioethanol-production/

2.5.1 Metal Oxides

Metal oxides are one form of a solid acid catalyst. As the name suggests, these catalysts are formed from chemical compounds built of at least one metal element and at least one oxygen atom. They have a high number of Lewis acid sites and are designed/prepared to have a high specific surface area and large porous sites.[11] The larger porous sites enable the reactants to contact the Lewis acid sites. Metal oxides have been used for the hydrolysis of sucrose, cellobiose, and cellulose.[11] An example of a metal oxide SAC is the layered transition-metal oxide, $HNbMoO_6$.[23] The metal oxide was able to hydrolyze sucrose, cellobiose, starch, and cellulose and found to exhibit a high level of activity thanks to its strong acidity, resistance to water, and intercalation ability.[11] Intercalation refers to the insertion of a molecule or ion into a layered structure.[24] When compared to Amberlyst-15, a polymer based acid catalyst which is discussed later, it produced glucose at twice the rate.[11] Nanoscale metal oxide catalysts are also being researched as potential SAC's.

2.5.2 Sulfonated Carbonaceous Based Acids

Sulfonated carbonaceous based acids are another form of an SAC which is being explored. These catalysts can be formed through two methods. One method, through the sulfonation of aromatic incompletely carbonized natural polymers such as sugars, cellulose, or starch.[11] Sulfonation refers to the process of substituting a sulfonic acid functional group onto an aromatic ring.[25] Second, the incomplete carbonization of sulfopolycyclic aromatic compounds. Compared to other SAC's, these catalysts have demonstrated superior activity when it comes to the hydrolysis

[23] A. Takagaki, C. Tagusagawa and K. Domen, Chem. Commun., 2008, 5363.
[24] Whittingham, M. S., & Jacobson, A. J. (1982). *Intercalation chemistry*. New York: Academic Press.
[25] Hunt, D. (n.d.). Sulfonation of Benzene. Retrieved from http://www.chem.ucalgary.ca/courses/351/Carey5th/Ch12/ch12-4.html

of cellulose. Moreover, this form of an SAC can be produced from raw materials and are easily recyclable. Hara reported the first carbonaceous acids from sulfonated d-glucose and sucrose through their incomplete carbonization followed by sulfonation.[11] A Brunauer-Emmett-Teller, BET, analysis revealed that the surface area of the catalyst during hydrolysis was about 560 m^2/g and then only 2 m^2/g following hydrolysis.[11] Compared to the hydrolysis of cellulose through other SAC's, the catalyst performed well. After three hours of reacting with cellulose, 68% of the cellulose was hydrolyzed to glucose, 4% yield, and soluble beta-1,4-glucan, 64% yield.[11] This outperformed liquid sulfuric acid. Moreover, the activation energy for the hydrolysis of cellulose was 110 kJ/mol as opposed to the 170 kJ/mol for liquid sulfuric acid.[11] This lower activation energy is accredited to the hydrogen bond interactions between the oxygen atoms in the glycosidic bonds of the beta-1,4-glucan and then phenolic OH groups of the catalyst. These interactions bind the cellulose to the surface of the catalyst, where it is then easier for the hydrolysis to take place. Impressively, this SAC was recovered from the reaction solution and reused at least 25 times without a decrease in activity and only 1% of the $-SO_3H$ groups separated into the solution.[11] This type of SAC provides a cheap and efficient option moving forward with the use of SAC's.

2.5.3 Heteropoly Acids

Heteropoly acids (HPAs) are a form of SAC made up of early transition metal-oxygen anion clusters. Often used in chemical transformations, the most utilized of these acids are Keggin type acids which have the formula $XY_xM_{(12-x)}O_{40}$ where X is the heteroatom and M and Y are addendum aoms.[11] However, these acids cannot be used as heterogeneous catalysts in polar solvents. Shimizu reported the use of $H_3PW_{12}O_{40}$ as a catalyst for the hydrolysis of cellobiose and

ball-milled cellulose into glucose or sugars.[26] Compared to mineral acids, the heteropoly acid demonstrated better hydrolysis activity with the sugar yield reducing in the following order from greatest yield to lowest yield: $H_3PW_{12}O_{40}$, $HSiW_{12}O_{40}$, $HClO_4$, H_2SO_4, H_3PO_4. Wang then optimized the hydrolysis reaction by using microcrystalline cellulose as the starting material, resulting in a glucose yield greater than 50% with a selectivity greater than 90%.[27] Moreover, the $H_3PW_{12}O_{40}$ was recovered from the solution using diethyl ether and lost on 8.8% of the total amount of starting material. The greatest glucose yield, 75.6%, was gathered by the Mu research group using 88% of $H_3PW_{12}O_{40}$ solution as a catalyst at 90°C for 3 hours under microwave irradiation.[28] The system was also used for the hydrolysis of lignocellulosic biomass and produced glucose yields of 37.2% for corncob, 43.3% for corn stover, and 27.8% for bagasse. There are other forms of HPAs which could be examined, but for the purpose of this paper we will not commit more time.

2.5.4 H-form Zeolites

H-form zeolites are another form of SAC which has been the subject of research. Zeolites are aluminosilicate minerals which are non-toxic and easily recovered from solutions.[29] Their microporous structure can accept different cations onto its structure, such as H^+, which is responsible for the catalytic activity of the compound. The acidity of the zeolite is determined by the ratio of Si:Al, where the number of Al atoms is equivalent to the number of Brønsted acid sites.[11] Moreover, the higher the Si:Al ratio the more hydrophobic these zeolites behave.

[26] K. Shimizu, H. Furukawa, N. Kobayashi, Y. Itayab and A. Satsuma, Green Chem., 2009, 11, 1627.
[27] J. Tian, J. Wang, S. Zhao, C. Jiang, X. Zhang and X. Wang, Cellulose, 2010, 17, 587.
[28] X. Li, Y. Jiang, L. Wang, L. Meng, W. Wang and X. Mu, RSC Adv., 2012, 2, 6921.
[29] Price, G. L. (n.d.). What is a Zeolite? Retrieved from http://www.personal.utulsa.edu/~geoffrey-price/zeolite/zeo_narr.htm

Compared to other forms of SAC's, H-form zeolites produce a low yield of glucose recovery under typical conditions. However, the use of microwave irradiation (MI) was found to increase the glucose yield.[11] In addition, lower yields of glucose were found to result as the degree of polymerization of cellulose increased. Table 1 below shows the performance of different H-form zeolites as solid acid catalysts.

Entry	Catalyst	Time/min	Yield of glucose	Yields of TRS
1[b]	HY	600	2.1	7.1
2[c]	HY	4	20.8	23.4
3	HY	8	36.9	47.5
4[d]	HY	15	24.2	34.8
5	HZSM-5a	9.5	35.2	42.9
6	HZSM-5b	9.5	33.7	45.3
7	H-beta	8.5	29.6	41.1
8	NKC-9	3.3	26.9	38.4
9[f]	HY	8	4.5	12.7
10	—	8	7.1	18.8

[a] Conditions: cellulose 100 mg, [C4mim]Cl 2.0 g, H_2O 10 ml, catalyst 10 mg, MI at 240 W. [b] Heated with an oil bath at 100 °C. [c] With MI at 400 W. [d] With MI at 80 W. [f] Heated with an oil bath at 180 °C.

Table 1: The results of solid acid-catalyzed hydrolysis of Avicel cellulose.[14]

2.5.5 Magnetic Solid Acids

One of the problems that occurs from the use of SAC's is the difficulty involved in separating the SAC's from solid residues that form during hydrolysis. While the cellulose is converted into soluble sugars, solid residues in the form of lignin components from the biomass and humins can form throughout the process which are challenging to separate from the recovered SAC's.[11] One of the main benefits of using SAC's is the potential to recover it from the process, so it's crucial to research this characteristic. Magnetic SAC's have been researched as a potential solution to this problem.

For example, Lai and Deng developed a magnetic sulfonated mesoporous silica (SBA-15) which could be separated from the system with a permanent magnet.[30,31] The SAC includes Fe_3O_4 magnetic particles along with sulfonic acid groups, SO_3H, making the complete compound Fe_3O_4-SBA-SO_3H. It produced a 50% yield of glucose for the hydrolysis of amorphous cellulose and a 25% yield for the hydrolysis of microcrystalline cellulose. In addition, as shown in Figure 4 below, it was shown to demonstrate a better hydrolysis performance than other SAC's at the same conditions.

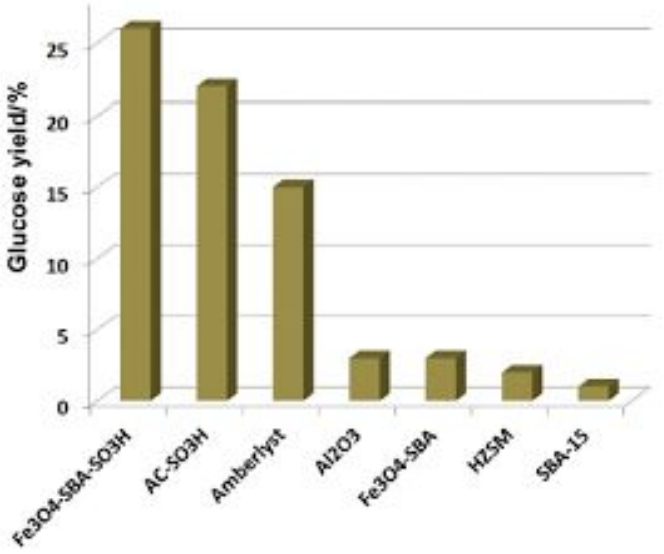

Figure 4: Hydrolysis of macrocrystalline cellulose by different solid acids (1.5 g solid acid catalyst, 1.5 g cellulose, 15 ml H_2O at 150℃ for 3 h).[14]

2.5.6 Supported Metal Catalysts

Supported metal catalysts have also been research as potential SAC's as a result of their superb hydrogenation activity. Extensive research has been focused on the conversion of cellulose into sugar alcohols through the use of a supported metal catalyst in the presence of acids.[11] However, the hydrolysis of cellulose to glucose is rarely accomplished by only supported metal catalysts

[30]D. Lai, L. Deng, Q. Guo and Y. Fu, Energy Environ. Sci., 2011, 4, 3552.
[31] D. Lai, L. Deng, J. Li, B. Liao, Q. Guo and Y. Fu, Chem-SusChem, 2011, 4, 55.

and the presence of acids still presents the issue of reactor corrosion. Of the supported metal catalysts being researched, Fukuoka demonstrated that the mesoporous carbon materials supported Ru catalyst (Ru/CMK-3) provided the greatest performance when compared to carbon black (XC-72), activated carbon (AC), and C_{60}.[11,32] While the CMK-3 was capable of converting cellulose to oligosaccharides and sugars by itself, the Ru was found to take an important role in the conversion of oligosaccharides into glucose. At 503 K, the CMK-3 produced a 21% yield of glucose and 22% yield of oligosaccharides. When the Ru loading ranged from 2% to 10%, the glucose yield increased from 28% to 34% while the oligosaccharide yield dropped from 22% to 5%.[11] Figure 5 below demonstrates the proposed mechanism for the hydrolysis of cellulose by Ru/CMK-3.

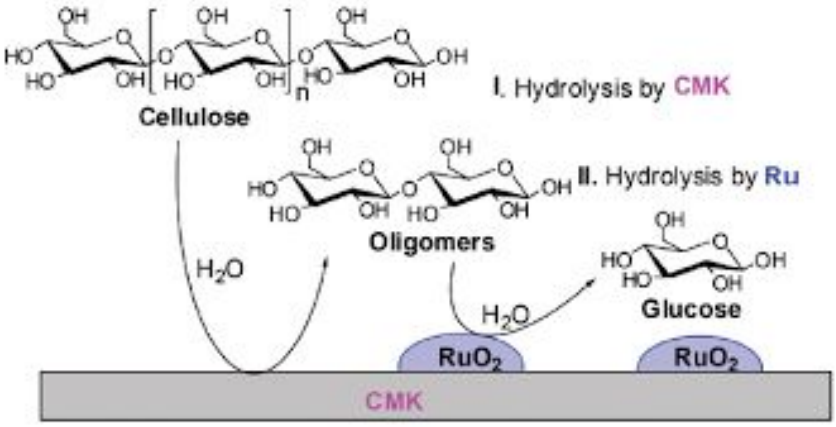

Figure 5: Hydrolysis of cellulose by Ru/CMK-3.[14]

2.5.7 Polymer Based Acids and the Scope of this Project

The main type of SACs this research is focused on are polymer based acids. They contain a number of Brønsted acid sites and have been used as an effective catalysts for multiple reactions including hydrolysis. One of the most well known of these is macroreticulated

[32] H. Kobayashi, T. Komanoya, K. Hara and A. Fukuoka, ChemSusChem, 2010, 3, 440.

styrene-divinylbenzene resins with sulfonic groups, known as Amberlyst. Amberlyst is commercially available, inexpensive, stable in most solvents, and macroporous to allow small molecules to interact with the acid sites within the pores.

Pan's research group created an ideal cellulose catalyst built up of a cellulose-binding domain and a catalytic domain.[11,33] The cellulose-binding domain was constructed from a chlorine group and the catalytic domain used a sulfonic acid group. Both of the groups were substituted onto a polystyrene compound so the chloromethyl polystyrene resin is the support group, with the sulfonic acid as the hydrolysis inductor. It is therefore notated as CP-SO_3H. Figure 6 illustrates the mechanism for cellulose hydrolysis.

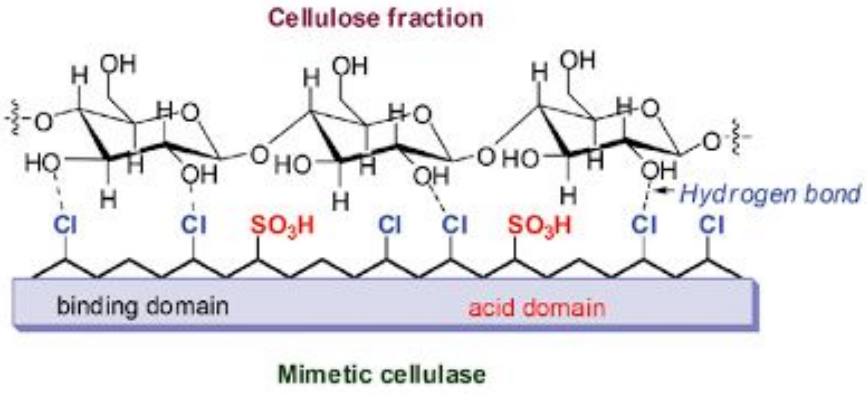

Figure 6: Hydrolysis mechanism of a cellulase-mimetic solid catalyst.[14]

CP-SO_3H was applied for the hydrolysis of cellobiose at 120°C. Over two hours, the cellobiose was completely hydrolyzed to glucose while only 8% of cellobiose was converted with sulfuric acid at the same conditions. In addition, the best yield of glucose, 93%, from this catalyst was

[33] Shuai, L., & Pan, X. (2012). Hydrolysis of cellulose by cellulase-mimetic solid catalyst. *Energy & Environmental Science,* (5), 6889-6894. doi:10.1039/C2EE03373A

observed from the hydrolysis of crystalline cellulose, also known as Avicel. While sulfuric acid hydrolyzed almost no Avicel. One of the most important aspects of this catalyst was the preferable adsorption of cellobiose over glucose. While experiments showed that both glucose and cellobiose were adsorbed, the preferable adsorption of cellobiose assures the desorption of glucose from the catalyst. Figure 7 below illustrates the adsorption of glucose and cellobioise onto different polymer based acids.

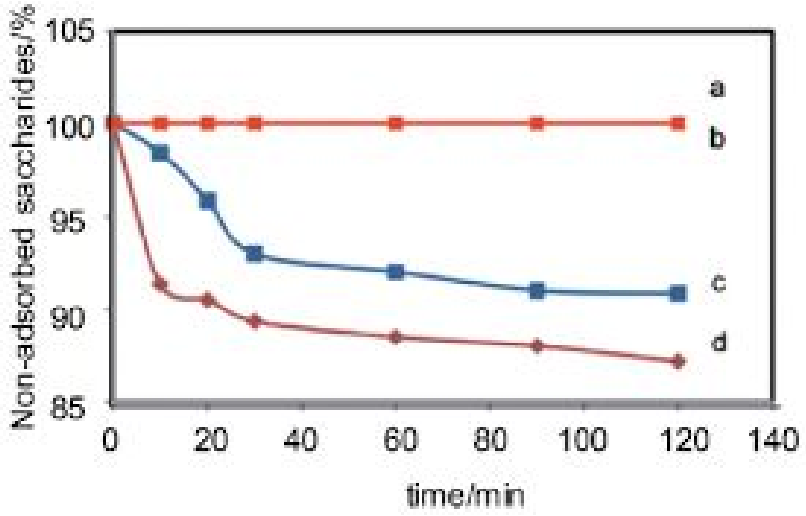

Figure 7: Adsorption curve of glucose and cellobiose onto resins in aqueous solution (a) glucose on Amberlyst-15; (b) cellobiose on Amberlyst-15; (c) glucose on CP–SO3H; and (d) cellobiose on CP–SO3H.[14]

In addition, the activation energy for cellulose hydrolysis when catalyzed by CP-SO_3H was 83 kJ/mol at 373-413 K. This activation energy is less than half of the activation energy for sulfuric acid at the same condition, 170-180 kJ/mol, and lower than that of the sulfonated active carbon (AC-SO_3H), 110 kJ/mol. This indicates that the hydrolysis reaction can be conducted at lower

temperatures. However, it is higher than the activation energy for enzymatic hydrolysis, 3-50 kJ/mol.

Overall, each SAC has its positive and negative characteristics. More research will need to be conducted into each type of catalyst and more compounds will need to be developed to better understand the potential mechanisms for hydrolysis. Table 2 below provides a comparison of the various catalysts which have been researched already. From the table, you can see that the CP-SO_3H has demonstrated superior cellulose conversion when compared to other methods. For this reason, our project researched a similar compound to see if it would exhibit the same performance.

Catalyst	Acidity (mmol g^{-1})	Pretreatment method	Solvents	Assistance method	Temp. (K)	Time (h)	Glucose and TRS[a] yield/%	Ref.
$HNbMoO_6$	1.90	—	H_2O	—	403	12	8.5	63
Zn–Ca–Fe	—	—	H_2O	—	433	20	29	64
Amberlyst-15	—	—	[BMIm]Cl/H_2O		373	5	11	68
CP-SO_3H	0.067	—	H_2O		393	10	93	74
Nafion NR50	—	[BMIm]Cl	H_2O		403	2	35	76
Nafion SAC50	—	—	H_2O		463	24	11	77
PCPs-SO_3H	1.80	—	H_2O	—	393	3	5.3	78
AC-SO_3H	1.90	—	H_2O	—	373	3	64	75
BC-SO_3H	1.98	—	H_2O	Microwave	363	1	19.8	83
CSA-SO_3H[b]	1.76	Milled/sieved	H_2O	Microwave	403	1	34.6	84
SC-SO_3H	2.15		[BMIm]Cl/H_2O	—	383	4	63	85
AC-N-SO_3H-250	2.23	Milled	H_2O	—	423	24	62.6	86
CMK-3-SO_3H	2.39	Milled	H_2O	—	423	24	74.5	86
Si_xC_y-SO_3H	0.37	Milled	H_2O	—	423	24	50.4	87
$H_3PW_{12}O_{40}$	—	Milled	H_2O	—	423	2	18	97
$H_3PW_{12}O_{40}$	—	—	H_2O	—	453	2	50.5	98
$H_3BW_{12}O_{40}$	—	—	H_2O	—	333	6	77	99
$H_3PW_{12}O_{40}$	—	Milled	H_2O	Microwave	363	3	75.6	100
Micellar HPA	—	—	H_2O	—	443	8	39.3	101
$[MIMPSH]_xH_{3-x}PW$	—	—	H_2O/MIBK	—	413	5	36	102
$CsH_2PW_{12}O_{40}$	—	—	H_2O	—	433	6	27	103
H-beta	1.05	Milled	H_2O	—	423	24	12	105
HY zeolite	—	Milled	[C_6mim]Cl/H_2O	Microwave	373	0.13	37	106
HY zeolite	1.36	—	[BMIm]Cl/H_2O	—	403	2	50	107
Fe_3O_4-SBA-SO_3H	1.09	—	H_2O	—	423	3	26	108
Fe_3O_4-SBA-SO_3H	1.09	Solvent activation	H_2O	—	423	3	50	108
MNPs@SiO_2-SO_3H	0.5	—	H_2O	—	423	3	30.2	112
Ru/CMK-3	—	Milled	H_2O	—	503	24	34.2	116
$CaFe_2O_4$	0.068	Milled	H_2O	—	423	24	36	117
HT-OH_{Ca}	1.17	Milled	H_2O	—	423	24	40.7	118

[a] TRS: total reducing sugars. [b] Corncob was used as the starting material.

Table 2: Different performances of solid acid catalysts in the hydrolysis of cellulose

Chapter 3: Methodology

3.1 Computational Methodology

One of the goals of this project was to observe the theoretical interactions between the two anomers of ringed glucose, alpha-D-glucose and beta-D-glucose, and two polymer based acids, 1-(chloromethyl)-4-methylbenzene and 1-hydroxymethyl-4-methylbenzene. Density-Functional Theory (DFT) software was utilized to simulate the theoretical absorption of the glucose anomers onto the polymer based acids through hydrogen bonding in a water solvent. To put it simply, DFT is a computational quantum mechanical method used to investigate the electronic structure of multiple-electron systems.[34] Walter Kohn shared the Nobel Prize for Theoretical Chemistry in 1998 for his development of the density-functional theory.[35] The theory was developed through observations of fundamental aspects of electronic structure theory such as the Schrödinger equation with the molecular Hamilton operator, antisymmetry of electronic wave function, the resulting Fermi correlation, the Slater determinant as a wave function for non-interaction fermions, and the Hartree-Fock approximation.[36] In the following sections we will describe the computational engine, DFT method, basis set, and calculation type we selected to complete our simulations.

[34] Cuevas, J. C. (n.d.). *Introduction to Density Functional Theory*. Lecture presented in Institut fur Theoretische Festkorperphysik Universitat Karlsruhe (Germany). Retrieved from https://www.uam.es/personal_pdi/ciencias/jcuevas/Talks/JC-Cuevas-DFT.pdf.

[35] Walter Kohn - Facts. (n.d.). Retrieved from https://www.nobelprize.org/nobel_prizes/chemistry/laureates/1998/kohn-facts.html

[36] Koch, W., & Holthausen, M. C. (2001). *A Chemist's Guide to Density Functional Theory* (Second ed.). Weinheim, Federal Republic of Germany: Wiley-VCH Verlag GmbH.

3.1.1 Computational Engine: Gaussian

A web-based interface, WebMo, was used to complete the computational simulations. The interface allows users to set-up, run, and visualize a number of chemical calculations with the freedom to choose certain job inputs which are dependent on the overall computational programs/engines. Our simulations were run using the Gaussian computational engine, Gaussian(R) 09. The program was originally released in 1970 by John Pople and his research group at Carnegie Mellon University, and has been updated periodically over the past 45+ years. [37] The name for the program originated from the use of Gaussian-type orbitals to speed up calculations compared to Slater-type orbitals, which were then operating on the limited computing power and hardware for Hartree-Fock calculations.

3.1.2 DFT Method

There are three types of density-functional methods: Local Density Approximation (LDA), Gradient Corrected (GC) methods, and hybrid methods. LDA methods assume that molecules have a uniform electron density throughout the system while GC methods aim to account for non-uniformity of electron density throughout a molecule.[28] Hybrid methods were developed to incorporate the useful aspects of LDA and GC methods. Most importantly, hybrid methods incorporate the Hartree-Fock exchange.[28] For this project, we utilized one of the most utilized hybrid method, B3LYP. Introduced by Stephens, Devlin, Chabalowski, and Frisch in 1994, the method is very similar to the original hybrid method introduced in 1993 by Axel Becke shown below in Equation 1.[28]

[37] Publisher's note: Sir John A. Pople, 1925-2004. (2004). *Journal of Computational Chemistry,25*(9). doi:10.1002/jcc.20049

$$\textit{Equation 1: } E_{XC}^{B3} = E_{XC}^{LSD} + a(E_{XC}^{\lambda=0} - E_{X}^{LSD}) + bE_{X}^{B} + cE_{C}^{PW91}$$

Where E_{XC}^{B3} represents the exchange-correlation energy, E_{XC}^{LSD} represents the local spin-density approximation energy, $E_{XC}^{\lambda=0}$ represents the exchange-correlation energy when the coupling strength parameter is equal to zero, E_{X}^{B} represents the exchange energy using the exchange functional developed by Becke, and E_{C}^{PW91} represents the correlation energy using the PW91 correlation functional developed by Perdew. The parameters a,b, and c are empirical parameters chosen so that the atomization and ionization energies as well as the proton affinities optimally reproduced the values in the G2 thermochemical data base: a=0.20, b=0.72, and c=0.81. Similar to the Becke's original hybrid method, the B3LYP is shown below in Equation 2. The a, b, and c parameters are taken directly from Becke's model. It's important to note that E_{X}^{B88} and E_{X}^{B} both represent the exchange energy from using Becke's exchange functional, the nomenclature can be found as both B88 and B. However, the B3LYP method replaces the PW91 correlation functional with the LYP functional.

$$\textit{Equation 2: } E_{XC}^{B3LYP} = (1-a)E_{X}^{LSD} + aE_{XC}^{\lambda=0} + bE_{X}^{B88} + cE_{C}^{LYP} + (1-c)E_{C}^{LSD}$$

The B3LYP method is regarded as the industry standard for practical applications. It's important to note that with respect to the G2 data base, there is an unsigned error of slightly above 2 kcal/mol.[28] However, this does not account for the basis set which was used in the computational models. The basis set described in the next section has a lower error.

3.1.3 Basis Set

When running a DFT computational calculation on Webmo, most methods require that a basis set be chosen. Essentially, a basis set is a collection of one-particle vector functions used to build the molecular orbitals.[38] Over the years, collections of basis sets have been constructed from wave function based approaches to quantum chemistry. Larger basis sets provide higher quality wave functions that account for electron correlation.[28] From the wave based functions, a configuration-interaction scheme consisting of a cartesian system of orbitals is used to model the molecules.[28] These basis sets are broken into different families such as Pople, Dunning, Karlsruhle, or Jensen depending on the orbital basis used in the collection.[39] The Gaussian basis set belongs to the Pople family because of its use of Pople-style orbitals which are also referred to as Gaussian-type orbitals. The orbital set, η^{GTO}, is expressed through Equation 3 below. This orbital set is usually referred to as a Gaussian primitive.

$$\textit{Equation 3: } \eta^{GTO} = N * x^L * y^m * z^n * exp(-\alpha * r^2)$$

"Where N is a normalization factor which ensures that $< \eta_\mu, \eta_\mu >= 1$. It's important to note that the η_μ are not orthogonal, perpendicular, i.e., $< \eta_\mu, \eta_\mu > \neq 0$ for $\mu \neq \nu$. α represents the orbital exponent which determines whether the resulting function or compact (large α) or diffusive (small α). L=1+m+n is used to classify the GTO as s-functions (L=O), p-functions (L=1), d-functions (L=2), etc. For L>1 the number of cartesian GTO functions exceeds the

[38] Sherrill, C. D. (n.d.). *Basis Sets in Quantum Chemistry*. Lecture presented in Georgia Institute of Technology: School of Chemistry and Biochemistry. Retrieved from http://vergil.chemistry.gatech.edu/courses/chem6485/pdf/basis-sets.pdf

[39] Basis Sets by Family. (n.d.). Retrieved from http://www.psicode.org/psi4manual/master/basissets_tables.html

number of $(2l+1)$ physical functions of angular momentum l. Similarly, the ten cartesian L=3 functions include an unwanted set of three p-type functions."[28]

Another type of orbital, the Slater-type orbital (STO), is theoretically viewed as a better choice for basis functions because STO's identically mimic the independent functions of the hydrogen. As opposed to GTO's, STO's illustrate a cusp behavior at r→0 while GTO's have a slope. Moreover, STO's demonstrate the desired exponential decay as r→∞ while GTO's decrease too rapidly. Equation 4 below shows how the orbital set is calculated.[28]

$$\textit{Equation 4:}\quad \eta^{STO} = N * r^{n-1} * exp(-\xi r) * Y_{lm}(\Theta, \phi)$$

Here, n represents the principal quantum number, the orbital exponent is differently represented as ξ, and Y_{lm} is the typical spherical harmonics that describe the angular part of the function. Unfortunately, STO basis sets are well-known for their difficulty in computations for many-center integrals because no analytical techniques exist. On the other hand, GTO basis functions have extremely efficient algorithms available for calculating the large amount of four-center-two-electron integrals. The many-center and four-center-two integrals refer to some of the calculations which make up the fundamentals of DFT such as the Coulomb contribution (Equation 5) and Hartree Fock exchange integral (Equation 6).[28]

$$\textit{Equation 5:}\quad J_{\mu\nu} = \sum_{\lambda}^{L}\sum_{\sigma}^{L} P_{\lambda\sigma} \iint \eta_{\mu}(\vec{r_1})\eta_{\nu}(\vec{r_1})\frac{1}{r_{12}}\eta_{\lambda}(\vec{r_2})\eta_{\sigma}(\vec{r_2})d\vec{r_1}d\vec{r_2}$$

Equation 6: $$K_{\mu\nu} = \sum_{\lambda}^{L}\sum_{\sigma}^{L} P_{\lambda\sigma}\iint \eta_{\mu}(x_1^{\rightarrow})\eta_{\lambda}(x_1^{\rightarrow})\frac{1}{r_{12}}\eta_{\nu}(x_2^{\rightarrow})\eta_{\sigma}(x_2^{\rightarrow})dx_1^{\rightarrow}dx_2^{\rightarrow}$$

To increase the accuracy of GTO basis functions, several Gaussian primitives are combined in a fixed linear combination to give one contracted Gaussian function (CGF) as shown in Equation 7 below.[28,40]

Equation 7: $$\eta_{\tau}^{CGF} = \sum_{a}^{A} d_{a\tau}\eta_{a}^{GTO}$$

Where $d_{a\tau}$ is chosen in a way that the CGF closely resembles a single STO function. The following figures illustrate the difference between STO and GTO functions, as well as how the CGF helps to eliminate these differences. Figure # below shows a comparison of STO and GTO functions with the same orbital exponent. The solid line represents STO and the dotted line, GTO.

[40] Standard, D. M. (n.d.). *Basis Set Notation*. Lecture presented at Chemistry 460 in Illinois State University, Normal, IL.

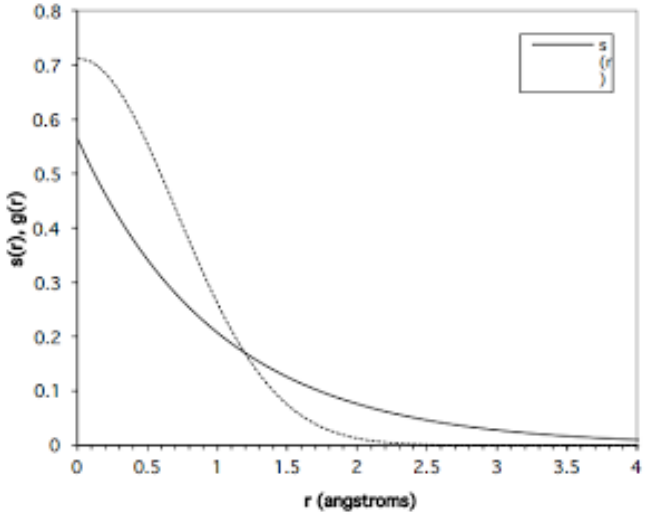

Figure 8: Comparison of Slater and Gaussian Type Orbitals. The orbital exponent for both is 1.0.[32]

As mentioned before, you can identify the favorable cusp behavior and exponential decay in the STO. This is why the CGF method is implemented. The figures below shows how the use of three Gaussian primitives with three different orbital exponents increases the accuracy of Gaussian methods. The first figure, Figure 9, illustrates three gaussian primitives: the solid line with $\alpha_1 = 1.0982 * 10^{-1}$, the dotted line with $\alpha_2 = 4.0577 * 10^{-1}$, and the dashed line with $\alpha_3 = 2.22766$. The second figure, Figure 10, represents the CGF of these three gaussian primitives and its comparison to the STO method. The coefficients used were $d_1 = 4.446 * 10^{-1}$, $d_2 = 5.353 * 10^{-1}$, and $d_3 = 1.543 * 10^{-1}$.[32]

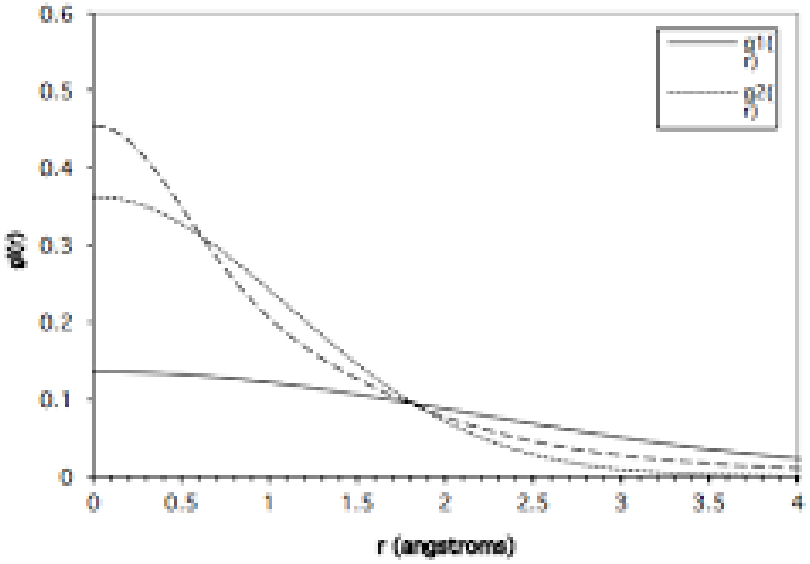

Figure 9: Plots of three gaussian primitive orbitals.[32]

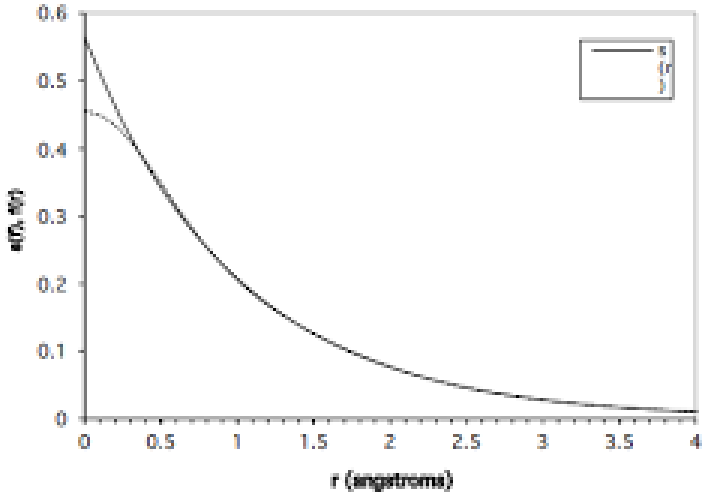

Figure 10: Construction of a basis function from the three orbitals shown in Fig. 9^ and comparison with the Slater Type Orbital of Fig. 10. [32]

Notice how in Figure 10, the CGF closely resembles the behavior of the STO despite missing the cusp at r→0. The basis set chosen for our computational calculations relies on this method to

improve the accuracy of our models. The specific basis set chosen and the calculation methods that construct it are discussed in the following section.

3.1.4 Defining 6-311+G(2d,p)

The basis set chosen to complete our computational models was Gaussian 6-311+G(2d,p). This basis set was chosen because of its higher level of accuracy as opposed to other basis sets and its shorter computational time when compared to the highest-accuracy basis sets. The notation indicates how the basis set is constructed.[32]

- 6= Number of gaussian primitives used to construct the core orbital basis function (the 1s function)
- 311= split valence triple zeta basis set
- 3= number of gaussian primitives used to construct the 2s and 2p basis functions
- 1= number of gaussian primitives used to construct the 2s' and 2p' basis functions
- 1= number of gaussian primitives used to construct the 2s'' and 2p'' basis functions
- + = means that one set of sp-type diffuse basis functions is added to non-hydrogen atoms (4 diffuse basis functions per atom)
- (2d,p) = 2 sets of d-type polarization functions are added to non-hydrogen atoms and 1 set of p-type polarization functions are added to hydrogen atoms

The 6 in the name represents the number of Gaussian primitives used to calculate the CGF for the core orbital basis function, the 1s function. Therefore, for our the 1s orbital calculations:

$$\eta_{\tau}^{CGF} = \sum_{a=1}^{a=6} d_{a\tau}\eta_{a}^{GTO}$$

311 represents the use of a split valence triple zeta basis set. Minimal basis sets consist of one basis function for each orbital whereas triple zeta basis employs three basis functions for each type of orbital. This means that for an orbital such as 2s, which only has one orbital function, would be analyzed three times as 2s, 2s', and 2s''. Similarly, the 2p orbital which consists of three different orbital functions, $2p_x$, $2p_y$, and $2p_z$, and is already analyzed with three times for each orbital function would be analyzed using a total of 9 basis functions in the form of 2p, 2p', and 2p''. The word split indicates that a minimal basis set would be implemented for the core electrons while a triple zeta set would be used on the valence electrons. So for a molecule with orbitals up to the 2p orbital system would implement a minimal basis set for the 1s orbital function, but three basis functions for the 2s and 2p orbitals. Likewise, a molecule with a 3p orbital system would apply a minimal basis set for 1s, 2s, and 2p and a triple set for the 3s and 3p orbitals.

The 3 indicates the number of gaussian primitives used to construct the 2s and 2p basis functions. The 1 following the 3 gives the number of gaussian primitives used to construct the 2s' and 2p' basis functions. The last 1 gives the number of gaussian primitives used to constructed the 2s'' and 2p'' basis functions.

The plus symbol, +, indicates that one set of sp-type diffuse basis functions is added to non-hydrogen atoms. This results in a total of 4 diffuse basis functions per atom, 1 from the s-type and 3 from the p-type. Diffuse basis functions are extra basis functions that are added to the basis set to represent broad electron distributions. As opposed to typical basis functions, diffuse basis functions have a much smaller orbital exponent, α. Diffuse basis functions are essential for representing anions or intermolecular systems, as is our case.

The (2d,p) represents that 2 sets of d-type polarization functions are added to non-hydrogen atoms and 1 set of p-type polarization functions are added to hydrogen atoms. Polarization functions are functions of higher angular momentum, l, than those occupied in the atom. For example, d-type functions for elements in the first row which only occupy s and p orbitals. As the name indicates, these functions are used to polarize the electron density within the molecule.

Knowing all of this, we can calculate the number of Gaussian primitives and basis functions which were used for each atom and molecule within our simulations, shown in Table 3.

Molecule	Total Primitives	Total Basis Functions
Glucose	600	420
1-chloromethyl-4-methylbenzene	462	327
1-hydroxymethyl-4-methylbenzene	458	321

Table 3: Gaussian primitives and basis functions for each atom and molecule simulated.

3.1.5 Calculation Type: Optimization + Vibrational Frequencies

Our simulation method chosen was the Optimization + Vibrational Frequencies job type. This job type first performs a geometry optimization calculation followed by a vibrational frequency calculation.[41] A geometry optimization calculation finds the nearest energy minimum by minimizing the energy of the system. Essentially what this means is that for a closed system, the internal energy of the system will minimize at equilibrium while the entropy of the surrounding system, the solvent, is maximized.[42] The vibrational frequencies calculation then finds the normal vibrational frequencies, intensities, and modes of the molecules in the system. The frequencies and intensities correlate to one another and are shown through an infrared spectrum in the results. You can modify the calculations to provide Raman spectrums as well. The modes of the molecules, refers to the motions by which the molecule vibrates. The frequencies and corresponding intensities provide an animation of the system at that condition which show the different modes. Modes can be shown as atoms swaying, ringed systems expanding and contracting in a breathing motion, or bond lengths stretching and retracting. Along with the vibrational frequencies, intensities and modes, the optimization and vibrational frequencies calculation provides the restricted energy, zero-pont energy, free energy, internal energy, enthalpy, constant volume specific heat, entropy, dipole moment, partial charges of each atom, bond lengths, and bond orders. The crucial value used in our adsorption calculations is the free energy.

[41] WebMO Help - Calculation Types. (n.d.). Retrieved from https://www.webmo.net/link/help/CalculationTypes.html

[42] *The Energy Minimum Principle*. (n.d.). Lecture presented at ESCI 341 - Lesson 11 in Millersville University, Millersville, PA. Retrieved from http://snowball.millersville.edu/~adecaria/ESCI341/esci341_lesson11_energy_minimum_principle.pdf

3.1.6 Adsorption Energy Calculation

From the computational simulations, we used the free energy values calculated from the models to calculate the adsorption energy of the glucose onto the two solid acid catalysts. The equation for calculating the adsorption energy is shown below as Equation 8.

$$\textit{Equation 8: } \Delta E = E_3 - (E_1 + E_2)$$

Where ΔE represents the adsorption energy, E_3 represents the energy values from the computational model including the glucose and the potential solid acid catalyst, E_1 represents the energy value from the model including only glucose, and E_2 represents the energy value from the model including only the solid acid catalyst. Each of the values were calculated using the same Optimization and Vibrational Frequency simulation with the 6-311+G(2d,p) basis set and water as the selected solvent.

3.2 Experimental Methodology

The other main objective of this project was to experimentally observe adsorption to polymer beads with the desired functional groups. To test this, glucose and cellobiose solutions were created in water and concentrations of 1, 4, 10, 20, and 30 grams of sugar per liter of solution (g/L) to be used in adsorption experiments. The adsorption experiments were conducted with hydroxymethyl styrene polymer beads in an effort to observe the interaction between glucose and cellobiose and the styrene monomer with a hydroxymethyl functional group, as was modeled in WebMo. In addition to the full description of the protocol for the adsorption experiments,

there are a number of minor experimental protocols discussed below that were related to, and led to, the main experiments.

3.2.1 Solution Preparation

Glucose solutions were created in deionized (DI) water at concentrations of 1, 4, 10, 20, and 30 g/L. The 30 g/L glucose solution was prepared by adding 1.2 grams of glucose to 40 mL, weighed to be 40.006 grams, of DI water. Two other 30 g/L stock solutions were created with 1.199 and 1.2008 grams of glucose and 40 mL, both weighed to be 40.009 grams, of DI water each to be diluted to the other desired concentrations. For the rest of the paper, the aforementioned 30 g/L stock solutions will be referred to as glucose stock 1 and glucose stock 2, respectively. As an example, for the 1 g/L glucose solution, 1.33 mL, weighed to be 1.3814 grams, of glucose stock 1 was mixed with 38.67 mL, weighed to be 38.6531 grams, of DI water. The rest of the information pertaining to the glucose solutions can be found in Appendix A in Tables 1.A and 2.A. These solutions were created assuming that the volume of the solution was equal to the volume of the water added.

Cellobiose solutions were created in DI water at concentrations of 1, 4, 10, 20, and 30 g/L. The 30 g/L cellobiose solution was prepared by adding 0.5999 grams of cellobiose to 20 mL, weighed to be 19.9949 grams, of DI water. Two other 30 g/L stock solutions were created with 0.6 and 0.6007 grams of cellulose and 20 mL, weighed at 20.0855 and 20.0412 grams respectively, of DI water each to be diluted to the other desired concentrations. For the rest of the paper, the aforementioned 30 g/L stock solutions will be referred to as cellobiose stock 1 and cellobiose stock 2, respectively. The other concentrations were derived similarly to the lower

concentration glucose solutions, as described above, and the information pertaining to the cellobiose solutions can be found in Appendix A in Table 3.A and 4.A. These solutions were created assuming that the volume of the solution was equal to the volume of the water added.

3.2.2 Preliminary Polymer Bead Tests

Before the adsorption experiments could begin, some preliminary testing was conducted on the polymer beads to be used in the experimentation. The two polymer beads that were studied in these experiments were chloromethyl styrene polymer beads (CMS PBs) and hydroxymethyl styrene polymer beads (HMS PBs). The first test was conducted on the CMS PBs and it was to establish if it were possible to substitute most if not all of the chloromethyl functional groups with hydroxymethyl functional groups. This experiment was conducted primarily because both PBs were observed to be hydrophobic, but literature suggested that the CMS PBs were more hydrophobic and, therefore, would be difficult to study with the resources available. Further, it would be easier to control the number of binding sites on the HMS PBs if they were synthesized in house. This substitution experiment was conducted by adding 5.1 grams of the CMS PBs to 15 mL of 1M NaOH solution, all within a sealed vial with a magnetic stir bar. The NaOH solution was prepared by adding 0.535 grams of 97% pure NaOH pellets to 15 mL of water. The vial was put in an oil bath on top of a magnetic hot plate and set at 150 ^{o}C and 150 rpm overnight. The following day the vial was removed from the oil bath, cooled, and its contents analyzed by raman spectroscopy to confirm if substitution had occurred. Because detecting hydroxymethyl groups via raman spectroscopy is difficult, the analysis was just to see if there were any differences in the intensity of the chloride peak of the spectra. A photo of the set up at the beginning of the experiment can be found in Figure 11 below.

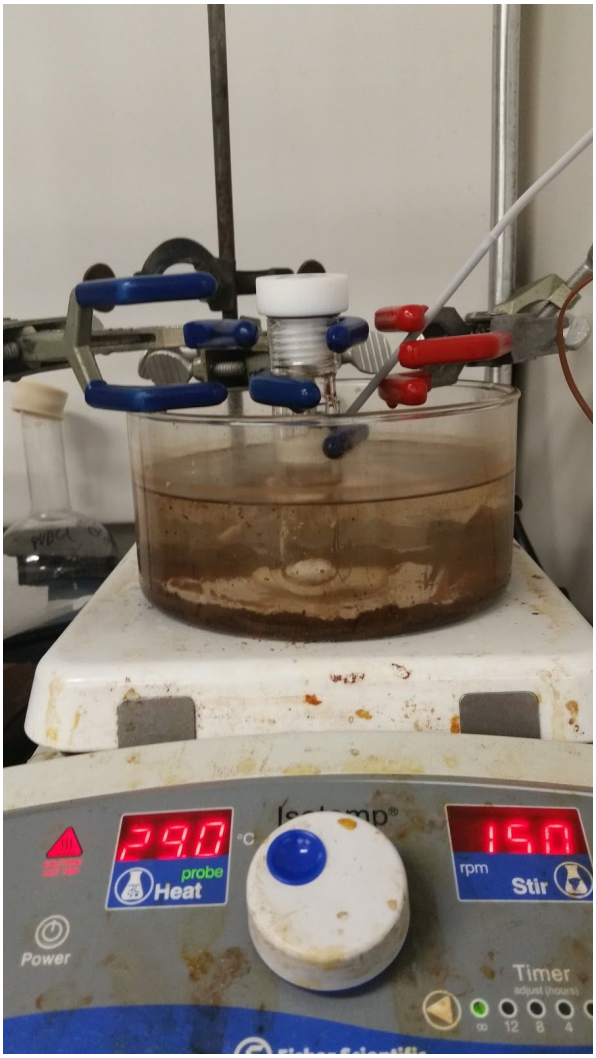

Figure 11: Substitution experiment setup with temperature probe coming from the upper left corner, vial in the center of the oil bath, and temperature and rpm gauge in the bottom of the photo

The next test was conducted on the HMS PBs and it was to find a solvent, or solution of multiple solvents, that could successfully disperse the PBs without excessive swelling. The following are the solvents and solutions tested, with all ratios being volume based: DI water, 1, 4-dioxane, ethanol, 50:50 water/dioxane, 50:50 water/ethanol, 80:20 water/dioxane, 80:20 water/ethanol, and 90:10 water/ethanol. This experimentation was fairly crude in that neither the total volumes

of nor the masses of HMS PBs added to the solutions were not exactly equal. Further, the analysis was qualitative in nature.

3.2.3 Adsorption Experiments

After preliminary testing and experimentation was completed, the adsorption experiments began. Three adsorption experiments were conducted in this project. The first adsorption experiment used the glucose solutions mixed with ethanol in a 90:10 volumetric ratio, respectively, with unaltered HMS PBs. Two controls were used in this experiment: a "blank" sample, which only had the 1 g/L glucose solution/ethanol mixture and no HMS PBs added, and a sample that replaced the HMS PBs with activated carbon, which also used the 1 g/L glucose solution/ethanol mixture. The second adsorption experiment used the glucose solutions without adding ethanol and used the HMS PBs after being ball milled for 10 minutes. The same controls were used in this second experiment as in the first, still without ethanol. The final adsorption experiment used the 1, 4, and 10 g/L cellobiose solutions and again used the 10 minute ball milled HMS PBs. The same two controls were employed for the cellobiose experiment, with the addition of a sample of 10 minute ball milled HMS PBs put in DI water instead of a cellobiose solution. This last control was added to observe a change in the results found in the second adsorption experiment, when the HMS PBs had been ball milled for the first time. The technique used to analyze the samples after adsorption was completed was high-performance liquid chromatography (HPLC) using an HPLC machine provided generously by Massachusetts Institute of Technology. To ensure the samples were at concentrations within the sensitivity of the HPLC instrument, while maintaining a basis by which adsorption can be observed if it occurred, all samples were diluted to 1 g/L after adsorption based on the original sugar solution concentration. All adsorption experiments were

run in triplicate. For the sake of reducing redundancy, only unique aspects of the experiments will be described in full below and all other relevant input data and calculations for these experiments can be found in Appendix A as Tables 3.A through 31.A.

Using the 30 g/L samples from the first adsorption experiment as an example, 0.9 mL of the solution were mixed with 0.1 mL of ethanol in a 0.5-dram glass vial and the masses were recorded. A new solution volume was calculated and recorded based on the volume of mixing relationship between water and ethanol shown in Figure 12 below, as adapted from the Dortmund Data Bank.

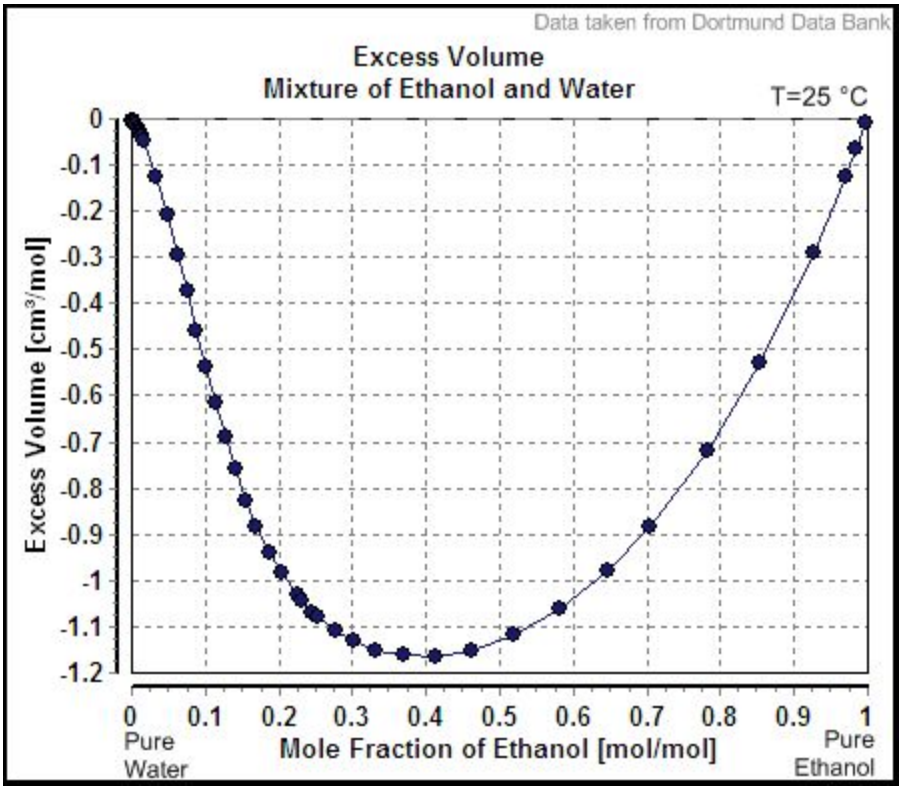

Figure 12: Excess Volume relationship of Ethanol and Water Mixtures

Subsequently, 0.1 grams of HMS PBs were added to the solution. The vial was left on a shaker table for 24 hours. This protocol was similar for the control vials: For the activated carbon control, 0.1 grams of activated carbon were added in the place of the HMS PBs; for the "blank" control, no adsorbing agent was added. Once the run was completed, the vial was taken off of the shaker table and the liquid was immediately separated from the HMS PBs using a needle and syringe and filtered out of the syringe into a separate 1 dram vial with a 0.2 micron filter. The separated and filtered solution was then diluted to approximately 1 g/L based on the original 30 g/L solution concentration. To do this, a 0.5 mL aliquot of the solution was taken, the mass was recorded, and 13.5 mL of DI water was added, again recording the mass. This protocol was repeated for the remaining glucose solutions with discrepancies only in the dilution step due to different amounts of DI water being needed for appropriate dilution. Further, the 1 g/L and control vials did not require further dilution. This protocol was also similar for the two other adsorption experiments, except 1 mL allotments of the sugar solutions were used instead of a 90:10 mixtures with ethanol and the HMS PBs were ball milled for 10 minutes before being used in the experiment. Further, the dilution was slightly different without ethanol in the mix. The only major differences in the cellobiose experiment were the lack of 20 and 30 g/L samples and that the third control group was added with 0.1 grams of 10 minute ball milled HMS PBs being added to 1 mL of DI water. These vials were all analyzed in the HPLC instrument, and the raw data from that was integrated by Maksim Tyufekchiev to find approximate glucose concentrations for each sample. These data were then analyzed to eventually find and plot approximate grams of sugar adsorbed per gram of HMS PBs. As mentioned above, all input data and calculated data for the adsorption experiments can be found in the appendix.

Chapter 4: Results and Discussion

4.1 Computational Results

Our computational simulations provided us with insight into whether or not the adsorption of glucose onto our polymer based acid was favorable. From the simulations, our adsorption energy values were calculated for the binding of glucose onto 1-chloromethyl-4-methylbenzene and 1-hydroxymethyl-4-methylbenzene. Hydrogen bonds were used to provide the binding interaction between the two compounds and glucose, Figure 13 illustrates the compounds and hydrogen bonds used in the simulations.

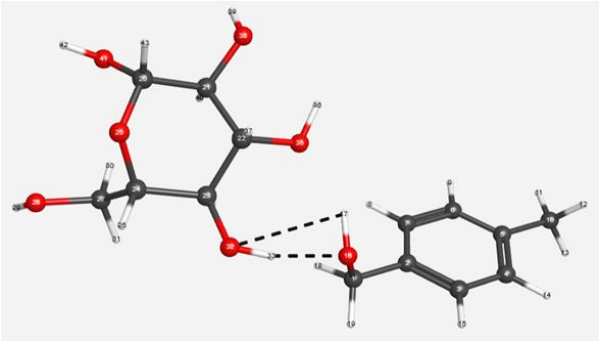

Figure 13: Examples of WebMO simulations for both functional groups

A total of ten simulations were run for each polymer based acid to account for the five potential binding sites, one for each hydroxyl functional group of glucose, and ten overall because of the two ringed isomers of glucose. Figure 14 below shows how the binding sites were labeled.

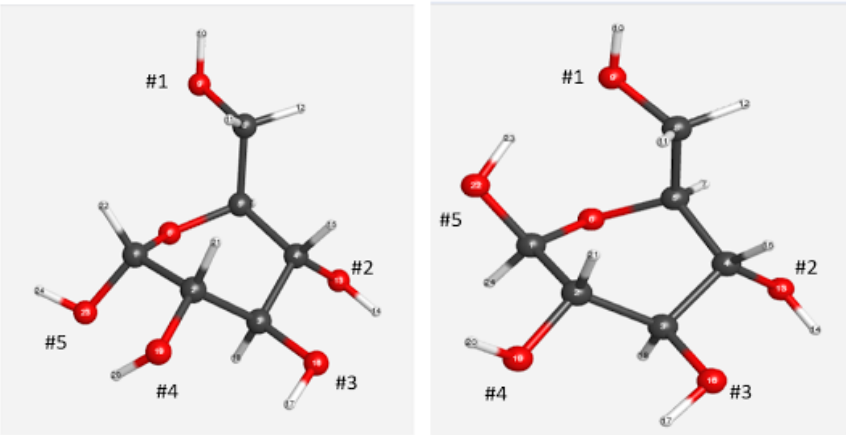

Figure 14: Alpha-D-Glucose and Beta-D-Glucose with labeled binding sites

From our adsorption energy calculations, we can determine that glucose is more favorably adsorbed onto the hydroxyl polymer based acid over the chloro polymer based acid. The hydroxy based acid produced some negative adsorption energy results, indicating that adsorption can occur spontaneously. On the other hand, the chloro based acid resulted in positive adsorption values which imply that some energy must be introduced into the system to induce adsorption. The results for the chloro based acid align with the expected result observed from the work by Pan's research group which stated that the polymer based acids needed to operate at higher temperatures than enzymatic hydrolysis. The simulations were conducted at 298 K, while Pan's research group conducted their experiments at 373-413 K. Moreover, Pan's research group determined that their CP-SO_3H catalyst more favorably adsorbed cellobiose than glucose. Unfortunately, attempts to simulate the adsorption of cellobiose onto both polymer based acids failed multiple times, thus preventing us from comparing the adsorption energy values of cellobiose and glucose. Figure 15 below provides a graph which compares the adsorption energy values for the the different binding sites, glucose isomers, and polymer based acids. The values

for each adsorption energy were assigned an unsigned error of about 2 kJ/mol in correlation to the basis set used for the simulations. (Basis Sets FAQ)

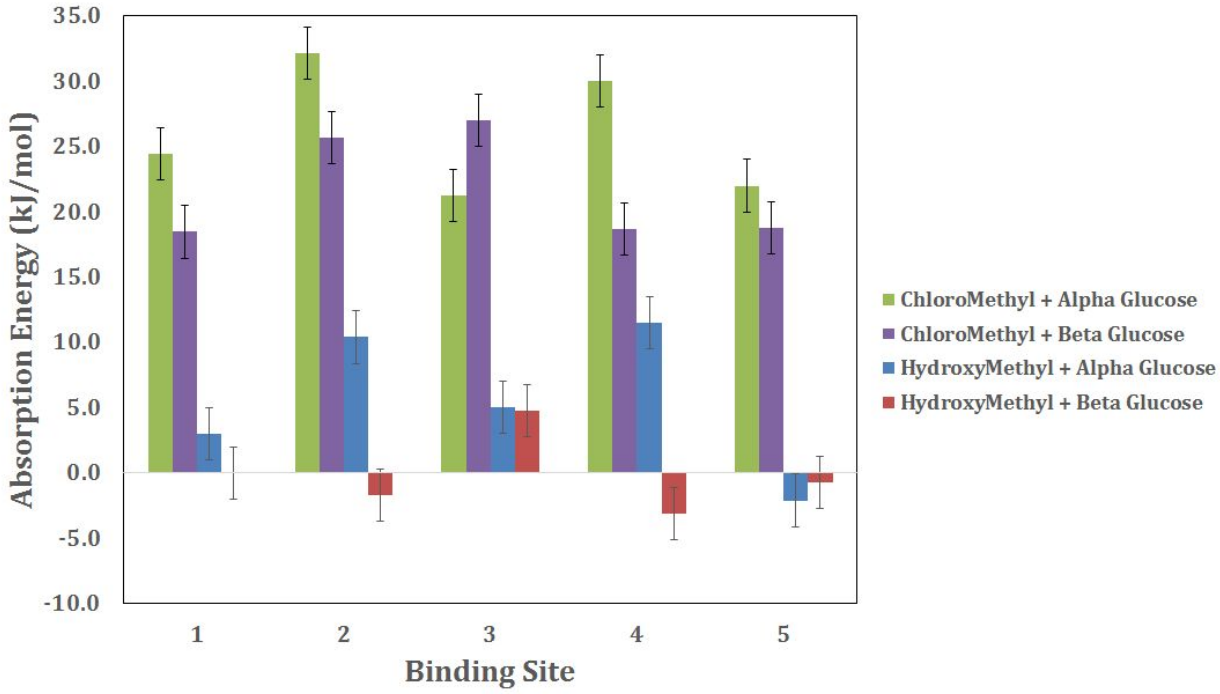

Figure 15: Comparison of adsorption energy values from computational results

The negative energies shown in the graph for the three binding sites with the hydroxymethyl based acid suggest that a spontaneous interaction between glucose and the hydroxymethyl functional group would occur. However, for the purpose of the binding domain in a solid acid catalyst, this spontaneity is not preferred. To obtain a higher yield of glucose, the binding domain should have a more favorable interaction with cellobiose or other more complex sugars so that they can interact with the catalytic domain and undergo hydrolysis while the produced glucose is free from the catalyst to move to fermentation. If glucose is binding with the solid acid then the hydrolysis will be limited and there will be a lower glucose yield. Fortunately, the adsorption

energy values are only slightly negative so the glucose binding is not extremely spontaneous, although it's likely to become more spontaneous with the higher temperatures that are associated with the hydrolysis process. Unfortunately, the simulations aimed at determining the adsorption energy with cellobiose failed multiple times so we were unable to compare the values to that of glucose. If the values for binding between the hydroxymethyl functional group and cellobiose were even more spontaneous than with glucose then hydroxymethyl could be considered a better binding domain than chloromethyl because it could operate at lower temperatures and have stronger hydrogen bonding. More computational modeling and research should be invested into determining whether the interaction between the hydroxymethyl binding domain and cellobiose is either less spontaneous or more spontaneous than binding with glucose.

4.2 Experimental Results

Each of the experiments pursued in the experimental lab work of this project were done so after being informed by literature and/or prior experimentation. Additionally, much of the initial computational results suggesting that there was no way to get glucose to interact with the chloromethyl styrene monomers suggested that time should not be spent trying to observe this phenomenon, or lack thereof, experimentally. The initial goal was to be able to substitute the chloromethyl groups on the CMS PBs with hydroxymethyl groups for a number of reasons, as described in the methodology. This level of control over the binding agents would have been helpful if more complex sugars were tested and appropriate solvents were found to test the CMS PBs.

4.2.1 Preliminary Polymer Bead Test Results

The attempts to substitute hydroxymethyl functional groups onto the CMS PBs were unsuccessful. Raman spectra of the reacted CMS PBs did not show significantly different chloride peaks. Rather than pursuing more sensitive analysis methods or more robust substitution methods, HMS PBs were used for the remainder of the experimentation. Where control over the exact composition of the polymer beads was lost, time was gained to be focused on adsorption experimentation instead.

After obtaining the HMS PBs from Sigma Aldrich, experiments were conducted to determine the best way to disperse the polymer beads in solution, since they are hydrophobic. As mentioned previously, this experimentation and analysis was fairly crude and qualitative in nature, with observations being made based on sight rather than any kind of quantitative or machine based analysis. As expected, the polymer beads remained at the top of the sample tested with pure DI water and there was no swelling, confirming the hydrophobic characteristics. Pure 1, 4-dioxane was conducive to the polymer beads dispersing in solution, but also appeared to swell the polymer beads significantly. This swelling was unfavorable for the experimentation that we wanted to conduct with the glucose solutions. Pure ethanol did not swell the polymer beads and, although there was some dispersion, the polymer beads primarily rested at the bottom of the liquid. Based on those first samples, the mixture samples were tested in 50:50 and 80:20 ratios were tested for water with both 1, 4-dioxane and ethanol. The dioxane mixtures still exhibited swelling beyond what was acceptable for the further experimentation and the ethanol mixtures showed better and better dispersion as the mixture included more water. Finally, a 90:10 ratio of

water to ethanol exhibited a favorable amount of dispersion, suggesting that the adsorption experiments would be more successful using this ratio of glucose solution to ethanol with the HMS PBs. Finding this ratio and the balance between dispersion and swelling, the adsorption experiments could proceed as described in the methodology.

4.2.2 Adsorption Experiments Results

Ultimately, only one of the three adsorption experiments seemed to show any adsorption happening. Regardless of this, the failed experiments informed and directed further experimentation as well as the conclusions and recommendations that are provided in the next and last section of this report. Further, in some ways the lack of adsorption did agree with the literature review that was conducted and in other ways prompted further literature review to inform more experimentation. In this sense, the main experiments of this project were largely exploratory and often elementary. Since so little research has been conducted to empirically determine the nature of the interaction between sugars and solid acid catalysts, there were only hypotheses and suggestions in literature to explore and pursue in this experimentation, and that is evident in the results of the experiments conducted. The first experiment conducted was with a 90:10 volumetric ratio of glucose solution to ethanol and 0.1 grams of HMS PBs, as well as that same mixture in a blank sample and a sample using activated carbons instead of polymer beads.

The first adsorption experiment was one of the three experiments to not show any adsorption. The notion that no adsorption occurred was confirmed by both of the control samples. All of the samples seemed to have the same resulting concentration of glucose, which was similar to the concentration detected in the blank sample. Further, regardless of if the polymer beads could

ever adsorb glucose, it is know based on past experimentation conducted by Maksim and generally in literature that activated carbons should be able to adsorb sugars. It was theorized that the interaction was hindered by the presence of ethanol and that the hydrophobic character of the polymer beads likely would not impede interaction since the samples were vigorously shaken on a shaker table for 24 hours. Based on those thoughts, the next adsorption experiment was altered to accommodate the appropriate changes. The only additional change, ball-milling the polymer beads for 10 minutes prior to experimentation, was decided on to further ensure that the polymer beads would disperse in solution so that the interaction could occur.

The second adsorption experiment was the one experiment to succeed in showing any adsorption of the sugar solution onto the polymer beads. Raw data from the HPLC analysis can be found in Tables 32.A-37.A in Appendix A. Approximate glucose concentrations of the resulting adsorbed solutions are shown in the bar graph below in Figure 16.

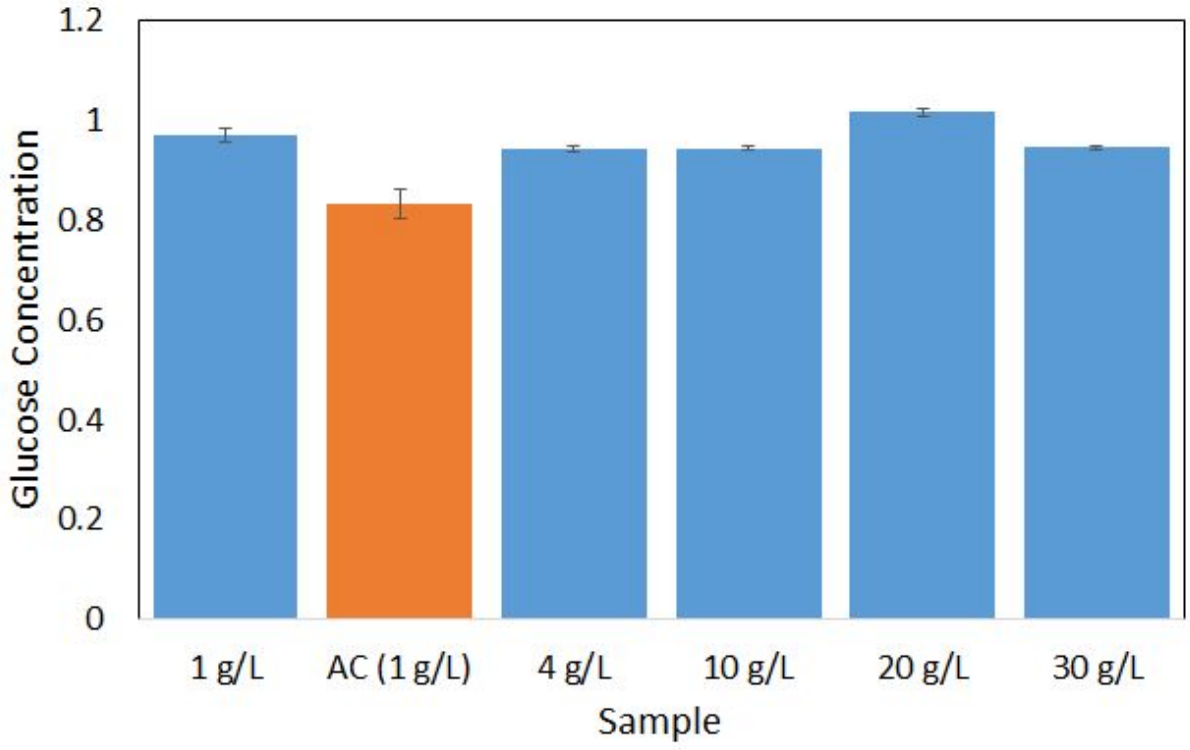

Figure 16: Glucose concentration of various samples based on HPLC analysis after adsorption

Additionally, Figure 17 shows a bar graph of the approximate grams of glucose adsorbed versus grams of polymer bead or activated carbon.

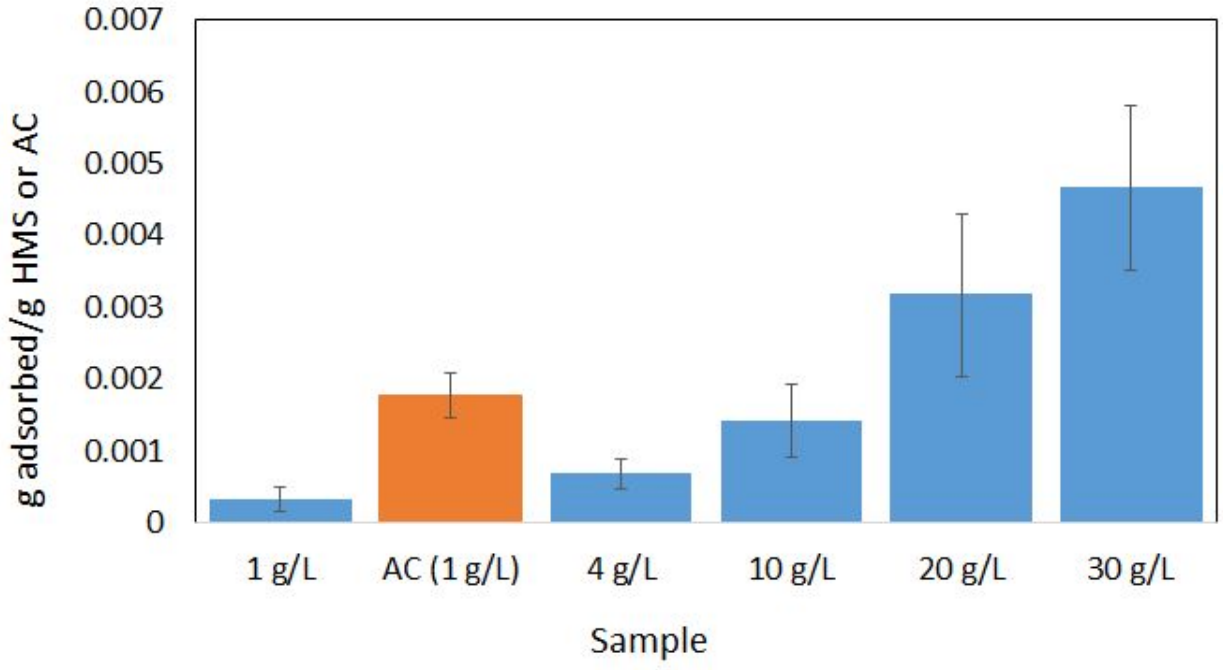

Figure 17: Mass of glucose adsorbed vs. mass of HMS PBs or activated carbon used for adsorption

These graphs clearly show that not only are the glucose concentrations lower in the samples with adsorbing agents in the total concentration of glucose observed, but they also show that the level of adsorption changes based on the original solution concentration. Further, the activated carbon mediated adsorption shows higher levels of adsorption than with the polymer beads, which was expected and important to observe. The only other notable, but unexpected, observation was a new peak showing up in the HPLC analysis. At this point, little thought was put into this mysterious peak because the adsorption that was expected was also observed, but it was something that was watched for in the last experiment. While it was positive to observe adsorption onto the HMS PBs because those results were in accordance with the computational results, this adsorption raised another issue that needed to be addressed: If glucose is adsorbing to the hydroxymethyl group, will that hinder adsorption of the longer chained sugars that need to be broken down for fermentation?

Given this thought, a more specific literature search was conducted to study research that has been conducted with solid acid catalysis that has high glucose yields after hydrolysis. Specifically, Huang et. al[6] conducted very successful experiments using polymer based solid acid catalysts, with glucose yields up to 93%, and they theorized about the interaction that was occurring. They hypothesized that the interaction was happening exclusively on or around the glycosidic bonds of the longer sugar chains as opposed to the individual units of the cellulose, meaning that the hydrolyzed glucose was free to flow out of the reaction without being held up by interacting with the catalyst. If true, this is an important aspect of the catalysts they employed because it means that less of the binding sites will be taken up, optimizing the hydrolysis, and the glucose yields can be has high as possible. However, they were using chloromethyl groups and the only polymers being tested in this project were the HMS PBs. So the questions remained about whether more cellobiose and other longer sugar chains would adsorb more than glucose and whether hydroxymethyl functional groups or chloromethyl functional groups are more suitable as binding agents in solid acid catalysis. These questions in some part informed the final adsorption experiment.

The third and final adsorption experiment, like the first, did not show adsorption. This was the most surprising result of the three, because it was expected that cellobiose would be more likely to adsorb onto the polymer beads. One explanation emerged that the mysterious peak that was observed in the second experiment was actually suggesting that the HMS PBs were somehow chemically changed after ball-milling, and that in this second batch of ball-milled polymer beads

they were more significantly changed and that restricted adsorption. Because the data were so different than expected and did not make much sense, they were not analyzed further and have not been included in this report. Regardless of these results, it is still likely that cellobiose would exhibit higher levels of adsorption onto the HMS PBs and important to show this difference to prove that hydroxymethyl groups are appropriate binding agents for solid acid catalysts.

Chapter 5: Conclusions and Recommendations

There are two main conclusions and recommendations for this project that will be described in depth below. The first recommendation is based on the analysis that was conducted and it is to conduct further research with different models, different polymer beads, and longer sugar chains. The second recommendation is based on what seems to be a lapse in the available research pertaining to solid acid catalysis. For solid acid catalysis to be commercialized and industrialized, research needs to be conducted into its techno-economic feasibility. Both of these recommendations have broad benefits for the future of solid acid catalysis as the chosen hydrolysis method of biofuel production, which is still in the formative stages of development. Before solid acid catalysis and biofuels can be seriously pursued and considered for mass production, they need to be properly vetted and determined to be viable options.

Based on the results of the computational and experimental analysis conducted on the interactions that glucose and cellobiose have with styrene derivatives with either hydroxymethyl or chloromethyl functional groups, the prevailing conclusion and recommendation of this project is to conduct further research. This project successfully observed adsorption of glucose on to hydroxymethyl styrene polymer beads both experimentally and computationally, but failed to observe any interactions with cellobiose rather than glucose. Further, although computational analysis was conducted to get an understanding of what happens between glucose and chloromethyl styrene, no lab experiments were conducted to back that up with the actual interaction. Finally, given the results from modeling of the interaction between glucose and hydroxymethyl styrene, it is now important to determine whether interactions with longer

chained sugars would be stronger or more favorable, as expected. If these interactions are stronger, the interaction between glucose and the binding site could be negligible in comparison meaning there would be no loss in glucose yield compared to the chloromethyl group. This largely unexplored area of research could greatly benefit solid acid catalysis to commercialize and industrialize this process for mass production.

These interactions are important to the optimization of solid acid catalyst for a number of reasons. First, it is necessary to conduct research to characterize the interaction to ensure that the best binding domain is employed on the catalyst. Further, it is important that whatever binding domain is ultimately used does not interact much with glucose so that glucose yields can remain as high as 93% has been seen in some of the literature. The easiest way to do that would be to ensure that the interaction happen on or near the glycosidic bonds, since those do not exist in glucose. Since this project was unable to successfully explore those longer sugar chains, and the experimentation does not exist yet in literature, it is important that the next step of this research be to better characterize the interaction.

Further work should be committed to developing a techno-economic analysis of the benefits of solid acid catalysts on an industrial scale. Throughout our research of solid acid catalysts, there was a noticeable lacking of journals and research pertaining to industrial scale operation. The significant portion of research was dedicated to lab-scale development of potential solid acid catalysts and their effectiveness as a hydrolysis agent, while any industrial pros and cons were merely speculation. To gain an understanding for how scaling up the use of these solid acid

catalysts will impact production, we recommend that pilot-scale lab experiments be conducted along with an economic analysis of industrial-scale yearly operations. This work will ultimately provide the crucial insight into whether or not solid acid catalysts are a viable replacement for enzymatic or dilute acid hydrolysis.

References

[1] Escobar, J. C., Lora, E. S., Venturini, O. J., Yanez, E. E., Castillo, E. F., & Almazan, O. (2009). Biofuels: Environment, technology and food security. *Renewable and Sustainable Energy Reviews, 13*, 1275-1287. doi:10.1016/j.rser.2008.08.014

[2] Doman, L. (2016, May 23). U.S. Energy Information Administration - EIA - Independent Statistics and Analysis. Retrieved April 23, 2017, from https://www.eia.gov/todayinenergy/detail.php?id=26352

[3] Xu, Z., & Huang, F. (2014). Pretreatment Methods for Bioethanol Production. *Applied Biochemistry and Biotechnology, 174*, 43-62. doi:10.1007/s12010-014-1015-y

[4] Guo, F., Fang, Z., Xu, C. C., & Smith, R. L. (2012). Solid acid mediated hydrolysis of biomass for producing biofuels. *Progress in Energy and Combustion Science, 38*(5), 672-690. doi:10.1016/j.pecs.2012.04.001

[5] Gupta, P., & Paul, S. (2014). Solid acids: Green alternatives for acid catalysis. *Catalysis Today, 236*, 153-170. doi:10.1016/j.cattod.2014.04.010

[6] Huang, Y., & Fu, Y. (2013). Hydrolysis of cellulose to glucose by solid acid catalysts. *Green Chemistry,* (5), 1095-1111. Retrieved from http://pubs.rsc.org/en/Content/ArticleLanding/2013/GC/c3gc40136g#!divAbstract

[7] Field, C., Campbell, J., & Lobell, D. (2008). Biomass energy: the scale of the potential resource. *Trends in Ecology & Evolution, 23*(2), 65-72. doi:10.1016/j.tree.2007.12.001

[8] Hoogwijk, M., Faaij, A., Broek, R. V., Berndes, G., Gielen, D., & Turkenburg, W. (2003). Exploration of the ranges of the global potential of biomass for energy. *Biomass and Bioenergy, 25*(2), 119-133. doi:10.1016/s0961-9534(02)00191-5

[9] Berndes, G., Hoogwijk, M., & van den Broek, R. (2003). The contribution of biomass in the future global energy supply: a review of 17 studies. *Biomass and bioenergy*, *25*(1), 1-28. doi: 10.1016/S0961-9534(02)00185-X

[10] Butera, G., De Pasquale, C., Maccotta, A., Alonzo, G., & Conte, P. (2011). Thermal transformation of micro-crystalline cellulose in phosphoric acid. *Cellulose*, *18*(6), 1499-1507. doi: 10.1007/s10570-011-9590-3

[11] O'sullivan, A. C. (1997). Cellulose: the structure slowly unravels. *Cellulose*, *4*(3), 173-207.

[12] Zhao, H., Kwak, J. H., Wang, Y., Franz, J. A., White, J. M., & Holladay, J. E. (2006). Effects of Crystallinity on Dilute Acid Hydrolysis of Cellulose by Cellulose Ball-Milling Study. *Energy & Fuels, 20*(2), 807-811. doi:10.1021/ef050319a

[13] First Generation Biofuels. (n.d.). Retrieved from http://biofuel.org.uk/first-generation-biofuel.html

[14] Second Generation Biofuels. (n.d.). Retrieved from http://biofuel.org.uk/second-generation-biofuels.html

[15] Third Generation Biofuels. (n.d.). Retrieved from http://biofuel.org.uk/third-generation-biofuels.html

[16] Murthy, G. S. (n.d.). *Cellulose, Hemicellulose and Lignin*. Lecture presented at Lecture Six in Oregon State University, Corvallis, OR. Retrieved from http://stl.bee.oregonstate.edu/courses/BFP/Class_Slides_W2011/BFP_Lecture6.pdf

[17] Blamire, J. (1999). The Giant Molecules of Life: Monomers and Polymers. Retrieved from http://www.brooklyn.cuny.edu/bc/ahp/SDPS/SD.PS.polymers.html

[18] Bioethanol: Production Processes. (n.d.). Retrieved from http://www.cropenergies.com/en/Bioethanol/Produktionsverfahren/

[19] Biofuel Production. (2007). *IEA Energy Technology Essentials,* 1-4. Retrieved from https://www.iea.org/publications/freepublications/publication/essentials2.pdf

[20] Sun, Y., & Cheng, J. (2002). Hydrolysis of lignocellulosic materials for ethanol production: a review. *Bioresource Technology,83*(1), 1-11. Retrieved from http://www.sciencedirect.com/science/article/pii/S0960852401002127

[21] Lin, Y., & Tanaka, S. (2006). Ethanol fermentation from biomass resources: current state and prospects. *Applied Microbiology and Biotechnology,69*(6), 627-642. Retrieved from https://link.springer.com/article/10.1007/s00253-005-0229-x

[22] Bioethanol Production. (n.d.). Retrieved from http://www.makebiofuel.co.uk/bioethanol-production/

[23] A. Takagaki, C. Tagusagawa and K. Domen, Chem. Commun., 2008, 5363.

[24] Whittingham, M. S., & Jacobson, A. J. (1982). *Intercalation chemistry*. New York: Academic Press.

[25] Hunt, D. (n.d.). Sulfonation of Benzene. Retrieved from http://www.chem.ucalgary.ca/courses/351/Carey5th/Ch12/ch12-4.html

[26] K. Shimizu, H. Furukawa, N. Kobayashi, Y. Itayab and A. Satsuma, Green Chem., 2009, 11, 1627.

[27] J. Tian, J. Wang, S. Zhao, C. Jiang, X. Zhang and X. Wang, Cellulose, 2010, 17, 587.

[28] X. Li, Y. Jiang, L. Wang, L. Meng, W. Wang and X. Mu, RSC Adv., 2012, 2, 6921.

[29] Price, G. L. (n.d.). What is a Zeolite? Retrieved from http://www.personal.utulsa.edu/~geoffrey-price/zeolite/zeo_narr.htm

[30] D. Lai, L. Deng, Q. Guo and Y. Fu, Energy Environ. Sci., 2011, 4, 3552.

[31] D. Lai, L. Deng, J. Li, B. Liao, Q. Guo and Y. Fu, Chem-SusChem, 2011, 4, 55.

[32] H. Kobayashi, T. Komanoya, K. Hara and A. Fukuoka, ChemSusChem, 2010, 3, 440.

[33] Shuai, L., & Pan, X. (2012). Hydrolysis of cellulose by cellulase-mimetic solid catalyst. *Energy & Environmental Science,* (5), 6889-6894. doi:10.1039/C2EE03373A

[34] Cuevas, J. C. (n.d.). *Introduction to Density Functional Theory*. Lecture presented in Institut fur Theoretische Festkorperphysik Universitat Karlsruhe (Germany). Retrieved from https://www.uam.es/personal_pdi/ciencias/jcuevas/Talks/JC-Cuevas-DFT.pdf

[35] Walter Kohn - Facts. (n.d.). Retrieved from https://www.nobelprize.org/nobel_prizes/chemistry/laureates/1998/kohn-facts.html

[36] Koch, W., & Holthausen, M. C. (2001). *A Chemist's Guide to Density Functional Theory* (Second ed.). Weinheim, Federal Republic of Germany: Wiley-VCH Verlag GmbH.

[37] Publisher's note: Sir John A. Pople, 1925-2004. (2004). *Journal of Computational Chemistry,25*(9). doi:10.1002/jcc.20049

[38] Sherrill, C. D. (n.d.). *Basis Sets in Quantum Chemistry*. Lecture presented in Georgia Institute of Technology: School of Chemistry and Biochemistry. Retrieved from http://vergil.chemistry.gatech.edu/courses/chem6485/pdf/basis-sets.pdf

[39] Basis Sets by Family. (n.d.). Retrieved from http://www.psicode.org/psi4manual/master/basissets_tables.html

[40] Standard, D. M. (n.d.). *Basis Set Notation*. Lecture presented at Chemistry 460 in Illinois State University, Normal, IL.

[41] WebMO Help - Calculation Types. (n.d.). Retrieved from https://www.webmo.net/link/help/CalculationTypes.html

[42] *The Energy Minimum Principle*. (n.d.). Lecture presented at ESCI 341 - Lesson 11 in Millersville University, Millersville, PA. Retrieved from http://snowball.millersville.edu/~adecaria/ESCI341/esci341_lesson11_energy_minimum_principle.pdf

Appendix A: Raw Data

30 g/L Glucose Solution Preparation			
	Stock 1	**Stock 2**	**Sample for Testing**
Mass of Glucose (g)	1.199	1.2008	1.2
Volume of Water (mL)	40	40	40
Mass of Water (g)	40.009	40.009	40.006
Concentration of Glucose (g/L)	29.975	30.02	30
Weight Fraction of Glucose (g Glucose/g Total)	0.02909629	0.0291387	0.029121973

Table 1.A: 30 g/L Glucose Solution Preparation input and calculated data

Other Glucose Solution Concentration Preparation				
	1 g/L	**4 g/L**	**10 g/L**	**20 g/L**
Volume of Stock Solution (mL)	1.33	5.33	13.33	26.67
Mass of Stock Solution (g)	1.3814	5.5183	13.7944	27.4052
Approximate Mass of Glucose (g)	0.04019362	0.16056207	0.40195088	0.7985519
Volume of Water (mL)	38.67	34.67	26.67	13.33
Mass of Water (g)	38.6531	34.6417	26.7002	13.3798
Concentration of Glucose (g/L)	1.00484044	4.0140517	10.0487721	19.9637975
Weight Fraction of Glucose (g/g)	0.00100397	0.00399806	0.00992604	0.01957955

Table 2.A: 1, 4, 10, and 20 g/L Glucose Solution Preparation input and calculated data

30 g/L Cellobiose Solution Preparation			
	Stock 1	**Stock 2**	**Sample for Testing**
Mass of Cellobiose (g)	0.5995	0.6007	0.5999
Volume of Water (mL)	20	20	20
Mass of Water (g)	20.0855	20.0412	19.9949
Concentration of Cellobiose (g/L)	29.975	30.035	29.995
Weight Fraction of Cellobiose (g Cellobiose/g Total)	0.02898235	0.029101	0.029128712

Table 3.A: 30 g/L Cellobiose Solution Preparation input and calculated data

Other Cellobiose Solution Concentration Preparation				
	1 g/L	**4 g/L**	**10 g/L**	**20 g/L**
Volume of Stock Solution (mL)	0.667	2.667	6.667	13.333
Mass of Stock Solution (g)	0.6736	2.6952	6.7521	13.5523
Approximate Mass of Cellobiose (g)	0.01959926	0.07842033	0.19649288	0.39277756
Volume of Water (mL)	19.333	17.333	13.333	6.667
Mass of Water (g)	19.1435	17.1887	13.272	6.6486
Concentration of Cellobiose (g/L)	0.97996311	3.92101631	9.82464422	19.6388781
Weight Fraction of Cellobiose (g/g)	0.00098901	0.00394391	0.00981282	0.01944357

Table 4.A: 1, 4, 10, and 20 g/L Cellobiose Solution Preparation input and calculated data

	1 g/L	AC (1 g/L)	Empty (1 g/L)
Volume of Ethanol (mL)	0.1	0.1	0.1
Mass of Ethanol (g)	0.076	0.0801	0.0803
Moles of Ethanol (mol)	0.001649719	0.001738717	0.001743059
Volume of Glucose Solution (mL)	0.9	0.9	0.9
Mass of Glucose Solution (mL)	0.898	0.8872	0.876
Mass of Glucose (g)	0.000901569	0.000890726	0.000879482
Moles of Glucose (mol)	5.00438E-06	4.9442E-06	4.88178E-06
Mass of Water (g)	0.897098431	0.886309274	0.875120518
Moles of Water (mol)	0.04979653	0.049197641	0.04857657
Total Moles of Mixture (mol)	0.051451254	0.050941302	0.050324511
Mole Fraction of Ethanol	0.032063736	0.034131782	0.034636378
Excess Mixture Volume (mL)	-0.006431407	-0.006367663	-0.006290564
Mixture Volume (mL)	0.993568593	0.993632337	0.993709436
New Glucose Concentration (g/L)	0.907405006	0.896434382	0.885049134
Final Ethanol Weight Fraction	0.078028747	0.082807816	0.083969466
Final Ethanol Concentration (g/L)	76	80.1	80.3

Table 5.A: 1 g/L, Activated Carbon, and Blank Glucose Sample 1 Experiment 1 Adsorption Preparation input and calculated data

	30 g/L	20 g/L	10 g/L	4 g/L
Volume of Ethanol (mL)	0.1	0.1	0.1	0.1
Mass of Ethanol (g)	0.0777	0.079	0.076	0.08
Moles of Ethanol (mol)	0.001686621	0.00171484	0.001649719	0.00173655
Volume of Solution (mL)	0.9	0.9	0.9	0.9
Mass of Solution (g)	0.9128	0.906	0.903	0.907
Mass of Glucose (g)	0.026582537	0.017739071	0.008950166	0.00366044
Moles of Glucose (mol)	0.000147553	9.84651E-05	4.96801E-05	2.0318E-05
Mass of Water (g)	0.886217463	0.888260929	0.894049834	0.90333956
Moles of Water (mol)	0.049192545	0.049305974	0.049627307	0.05014297
Total Moles of Mixture (mol)	0.051026719	0.051119279	0.051326707	0.05189983
Mole Fraction of Ethanol	0.033053684	0.033545855	0.03214154	0.03345958
Excess Mixture Volume (mL)	-0.00637834	-0.00638991	-0.006415838	-0.0064875
Mixture Volume (mL)	0.99362166	0.99361009	0.993584162	0.99351252
Glucose Concentration (g/L)	26.75317738	17.85315133	9.007959778	3.68433799
Ethanol Weight Fraction	0.07844523	0.080203046	0.077630235	0.0810537
Ethanol Concentration (g/L)	77.7	79	76	80

Table 6.A: 30, 20, 10, and 4 g/L Glucose Sample 1 Experiment 1 Adsorption Preparation input and calculated data

	30 g/L	20 g/L	10 g/L	4 g/L
Mixture Aliquot Taken Post Adsorption (mL)	0.5	0.5	0.5	0.5
Mass of Aliquot (g)	0.495	0.4971	0.4976	0.4856
Mass of Ethanol based on Original Concentration (g)	0.038830389	0.039868934	0.038628805	0.03935968
Mass of Glucose based on Original Concentration (g)	0.013376589	0.008926576	0.00450398	0.00184217
Volume of Water Added (mL)	13.5	8.6	4.2	1.4
Mass of Water Added (g)	13.4152	8.458	4.187	1.3967
New Glucose Concentration (g/L)	0.955470621	0.980942381	0.958293593	0.96956263
Final Ethanol Weight Fraction	0.002791505	0.004452093	0.008245913	0.02091042
Final Ethanol Concentration (g/L)	2.773599192	4.38120154	8.21889466	20.7156188

Table 7.A: 30, 20, 10, and 4 g/L Glucose Sample 1 Experiment 1 Dilution Preparation input and calculated data for HPLC Analysis

	1 g/L	AC (1 g/L)	Empty (1 g/L)
Volume of Ethanol (mL)	0.1	0.1	0.1
Mass of Ethanol (g)	0.0753	0.076	0.0767
Moles of Ethanol (mol)	0.001634525	0.001649719	0.001664914
Volume of Glucose Solution (mL)	0.9	0.9	0.9
Mass of Glucose Solution (mL)	0.9074	0.906	0.9071
Mass of Glucose (g)	0.000911006	0.000909601	0.000910705
Moles of Glucose (mol)	5.05677E-06	5.04897E-06	5.0551E-06
Mass of Water (g)	0.906488994	0.905090399	0.906189295
Moles of Water (mol)	0.050317785	0.050240152	0.05030115
Total Moles of Mixture (mol)	0.051957367	0.05189492	0.051971119
Mole Fraction of Ethanol	0.031458958	0.031789613	0.032035373
Excess Mixture Volume (mL)	-0.006494671	-0.006486865	-0.00649639
Mixture Volume (mL)	0.993505329	0.993513135	0.99350361
New Glucose Concentration (g/L)	0.916961841	0.915539895	0.916660266
Final Ethanol Weight Fraction	0.076625623	0.077393075	0.077963001
Final Ethanol Concentration (g/L)	75.3	76	76.7

Table 8.A: 1 g/L, Activated Carbon, and Blank Glucose Sample 2 Experiment 1 Adsorption Preparation input and calculated data

	30 g/L	20 g/L	10 g/L	4 g/L
Volume of Ethanol (mL)	0.1	0.1	0.1	0.1
Mass of Ethanol (g)	0.0807	0.0758	0.0795	0.0763
Moles of Ethanol (mol)	0.001751742	0.001645378	0.001725693	0.00165623
Volume of Solution (mL)	0.9	0.9	0.9	0.9
Mass of Solution (g)	0.915	0.9093	0.9087	0.9064
Mass of Glucose (g)	0.026646605	0.017803684	0.009006662	0.00365801
Moles of Glucose (mol)	0.000147909	9.88238E-05	4.99937E-05	2.0305E-05
Mass of Water (g)	0.888353395	0.891496316	0.899693338	0.90274199
Moles of Water (mol)	0.049311107	0.049485565	0.049940569	0.05010979
Total Moles of Mixture (mol)	0.051210757	0.051229767	0.051716256	0.05178633
Mole Fraction of Ethanol	0.034206515	0.032117617	0.033368489	0.03198202
Excess Mixture Volume (mL)	-0.006401345	-0.006403721	-0.006464532	-0.0064733
Mixture Volume (mL)	0.993598655	0.993596279	0.993535468	0.99352671
Glucose Concentration (g/L)	26.8182779	17.91842843	9.065264926	3.68184815
Ethanol Weight Fraction	0.081048509	0.076946503	0.080449302	0.07764323
Ethanol Concentration (g/L)	80.7	75.8	79.5	76.3

Table 9.A: 30, 20, 10, and 4 g/L Glucose Sample 2 Experiment 1 Adsorption Preparation input and calculated data

	30 g/L	20 g/L	10 g/L	4 g/L
Mixture Aliquot Taken Post Adsorption (mL)	0.5	0.5	0.5	0.5
Mass of Aliquot (g)	0.4918	0.4934	0.4892	0.4858
Mass of Ethanol based on Original Concentration (g)	0.039859657	0.037965405	0.039355798	0.03771908
Mass of Glucose based on Original Concentration (g)	0.013409139	0.008959214	0.004532632	0.00184092
Volume of Water Added (mL)	13.5	8.6	4.2	1.4
Mass of Water Added (g)	13.5294	8.6156	4.1994	1.3976
New Glucose Concentration (g/L)	0.957795639	0.984529034	0.964389886	0.96890741
Final Ethanol Weight Fraction	0.002842813	0.0041679	0.008393934	0.02002712
Final Ethanol Concentration (g/L)	2.847118323	4.172022476	8.373574132	19.8521474

Table 10.A: 30, 20, 10, and 4 g/L Glucose Sample 2 Experiment 1 Dilution Preparation input and calculated data for HPLC Analysis

	1 g/L	AC (1 g/L)	Empty (1 g/L)
Volume of Ethanol (mL)	0.1	0.1	0.1
Mass of Ethanol (g)	0.0815	0.0808	0.0815
Moles of Ethanol (mol)	0.00176911	0.00175391	0.00176911
Volume of Glucose Solution (mL)	0.9	0.9	0.9
Mass of Glucose Solution (mL)	0.9077	0.9078	0.9063
Mass of Glucose (g)	0.00091131	0.00091141	0.0009099
Moles of Glucose (mol)	5.0584E-06	5.059E-06	5.0506E-06
Mass of Water (g)	0.90678869	0.90688859	0.9053901
Moles of Water (mol)	0.05033442	0.05033997	0.05025679
Total Moles of Mixture (mol)	0.05210859	0.05209894	0.05203095
Mole Fraction of Ethanol	0.03395039	0.03366503	0.03400105
Excess Mixture Volume (mL)	-0.0065136	-0.0065124	-0.0065039
Mixture Volume (mL)	0.99348643	0.99348763	0.99349613
New Glucose Concentration (g/L)	0.91728245	0.9173824	0.91585873
Final Ethanol Weight Fraction	0.08238981	0.08173174	0.08250658
Final Ethanol Concentration (g/L)	81.5	80.8	81.5

Table 11.A: 1 g/L, Activated Carbon, and Blank Glucose Sample 3 Experiment 1 Adsorption Preparation input and calculated data

	30 g/L	20 g/L	10 g/L	4 g/L
Volume of Ethanol (mL)	0.1	0.1	0.1	0.1
Mass of Ethanol (g)	0.0769	0.0812	0.0827	0.0841
Moles of Ethanol (mol)	0.00166926	0.00176259	0.00179516	0.00182554
Volume of Solution (mL)	0.9	0.9	0.9	0.9
Mass of Solution (g)	0.9135	0.9065	0.9087	0.9072
Mass of Glucose (g)	0.02660292	0.01774886	0.00900666	0.00366124
Moles of Glucose (mol)	0.00014767	9.8519E-05	4.9994E-05	2.0323E-05
Mass of Water (g)	0.88689708	0.88875114	0.89969334	0.90353876
Moles of Water (mol)	0.04923027	0.04933318	0.04994057	0.05015402
Total Moles of Mixture (mol)	0.05104719	0.0511943	0.05178572	0.05199989
Mole Fraction of Ethanol	0.03270024	0.03442952	0.03466506	0.0351067
Excess Mixture Volume (mL)	-0.0063809	-0.0063993	-0.0064732	-0.0065
Mixture Volume (mL)	0.9936191	0.99360071	0.99352679	0.99350001
Glucose Concentration (g/L)	26.7737626	17.8631727	9.06534415	3.68519681
Ethanol Weight Fraction	0.0776454	0.0822112	0.08341739	0.08483809
Ethanol Concentration (g/L)	76.9	81.2	82.7	84.1

Table 12.A: 30, 20, 10, and 4 g/L Glucose Sample 3 Experiment 1 Adsorption Preparation input and calculated data

	30 g/L	20 g/L	10 g/L	4 g/L
Mixture Aliquot Taken Post Adsorption (mL)	0.5	0.76	0.5	0.5
Mass of Aliquot (g)	0.5018	0.7669	0.4965	0.4978
Mass of Ethanol based on Original Concentration (g)	0.03985966	0.03796541	0.0393558	0.03771908
Mass of Glucose based on Original Concentration (g)	0.01338688	0.01357601	0.00453267	0.0018426
Volume of Water Added (mL)	13.5	12	4.2	1.4
Mass of Water Added (g)	13.4703	11.96	4.1925	1.3856
New Glucose Concentration (g/L)	0.95620581	1.06395072	0.96439831	0.96978863
Final Ethanol Weight Fraction	0.0028528	0.00298308	0.00839322	0.02002712
Final Ethanol Concentration (g/L)	2.84711836	2.97534522	8.37357404	19.8521474

Table 13.A: 30, 20, 10, and 4 g/L Glucose Sample 3 Experiment 1 Dilution Preparation input and calculated data for HPLC Analysis

	1 g/L	AC (1 g/L)	Empty (1 g/L)
Volume of Glucose Solution (mL)	1	1	1
Mass of Glucose Solution (mL)	0.998	1.0106	1.0054
Mass of Glucose (g)	0.00100197	0.00101462	0.0010094
Moles of Glucose (mol)	5.5617E-06	5.6319E-06	5.6029E-06
Mass of Water (g)	0.99699803	1.00958538	1.0043906
Moles of Water (mol)	0.0553418	0.0560405	0.05575215
Glucose Concentration (g/L)	1.00196657	1.01461665	1.00939598

Table 14.A: 1 g/L, Activated Carbon, and Blank Glucose Sample 1 Experiment 2 Adsorption Preparation input and calculated data

	30 g/L	20 g/L	10 g/L	4 g/L
Volume of Solution (mL)	1	1	1	1
Mass of Solution (g)	1.0179	0.9937	1.0114	0.9798
Mass of Glucose (g)	0.02964326	0.0194562	0.01002458	0.00395424
Moles of Glucose (mol)	0.00016454	0.000108	5.5644E-05	2.1949E-05
Mass of Water (g)	0.98825674	0.9742438	1.00137542	0.97584576
Moles of Water (mol)	0.05485659	0.05407875	0.05558478	0.05416767
Glucose Concentration (g/L)	29.6432558	19.4561977	10.0245826	3.95423939

Table 15.A: 30, 20, 10, and 4 g/L Glucose Sample 1 Experiment 2 Adsorption Preparation input and calculated data

	30 g/L	20 g/L	10 g/L	4 g/L
Mixture Aliquot Taken Post Adsorption (mL)	0.5	0.5	0.5	0.5
Mass of Aliquot (g)	0.5039	0.502	0.4951	0.5015
Mass of Glucose based on Original Concentration (g)	0.01467456	0.00982893	0.00490723	0.00202393
Volume of Water Added (mL)	14.5	8.8	4.55	1.56
Mass of Water Added (g)	14.5059	8.8204	4.187	1.3967
New Glucose Concentration (g/L)	0.97830413	1.05687457	0.9717284	0.98249249

Table 16.A: 30, 20, 10, and 4 g/L Glucose Sample 1 Experiment 2 Dilution Preparation input and calculated data for HPLC Analysis

	1 g/L	AC (1 g/L)	Empty (1 g/L)
Volume of Glucose Solution (mL)	1	1	1
Mass of Glucose Solution (mL)	1.002	1.0046	0.9028
Mass of Glucose (g)	0.001005982	0.001008593	0.000906388
Moles of Glucose (mol)	5.58396E-06	5.59844E-06	5.03113E-06
Mass of Water (g)	1.000994018	1.003591407	0.901893612
Moles of Water (mol)	0.055563611	0.055707788	0.050062703
Glucose Concentration (g/L)	1.005982465	1.008592798	0.906388193

Table 17.A: 1 g/L, Activated Carbon, and Blank Glucose Sample 2 Experiment 2 Adsorption Preparation input and calculated data

	30 g/L	20 g/L	10 g/L	4 g/L
Volume of Solution (mL)	1	1	1	1
Mass of Solution (g)	0.9997	1.0154	1.012	1.0089
Mass of Glucose (g)	0.029113236	0.019881074	0.01003053	0.00407168
Moles of Glucose (mol)	0.0001616	0.000110355	5.56769E-05	2.26009E-05
Mass of Water (g)	0.970586764	0.995518926	1.00196947	1.00482832
Moles of Water (mol)	0.053875752	0.055259698	0.055617757	0.055776448
Glucose Concentration (g/L)	29.11323594	19.88107395	10.03052952	4.071680054

Table 18.A: 30, 20, 10, and 4 g/L Glucose Sample 2 Experiment 2 Adsorption Preparation input and calculated data

	30 g/L	20 g/L	10 g/L	4 g/L
Mixture Aliquot Taken Post Adsorption (mL)	0.5	0.5	0.5	0.5
Mass of Aliquot (g)	0.5007	0.4978	0.4996	0.4977
Mass of Glucose based on Original Concentration (g)	0.014581372	0.009746699	0.004951831	0.002008599
Volume of Water Added (mL)	14.5	8.8	4.55	1.56
Mass of Water Added (g)	14.5687	8.817	4.5415	1.5577
New Glucose Concentration (g/L)	0.972091443	1.048032198	0.980560511	0.975047881

Table 19.A: 30, 20, 10, and 4 g/L Glucose Sample 2 Experiment 2 Dilution Preparation input and calculated data for HPLC Analysis

	1 g/L	AC (1 g/L)	Empty (1 g/L)
Volume of Glucose Solution (mL)	1	1	1
Mass of Glucose Solution (mL)	0.9972	1.0091	1.0086
Mass of Glucose (g)	0.001001163	0.001013111	0.001012609
Moles of Glucose (mol)	5.55721E-06	5.62352E-06	5.62074E-06
Mass of Water (g)	0.996198837	1.008086889	1.007587391
Moles of Water (mol)	0.055297438	0.055957326	0.055929599
Glucose Concentration (g/L)	1.001163387	1.013110684	1.012608696

Table 20.A: 1 g/L, Activated Carbon, and Blank Glucose Sample 3 Experiment 2 Adsorption Preparation input and calculated data

	30 g/L	20 g/L	10 g/L	4 g/L
Volume of Solution (mL)	1	1	1	1
Mass of Solution (g)	1.0195	1.0152	1.0148	1.0091
Mass of Glucose (g)	0.029689851	0.019877158	0.010058282	0.00407249
Moles of Glucose (mol)	0.000164801	0.000110333	5.5831E-05	2.2605E-05
Mass of Water (g)	0.989810149	0.995322842	1.004741718	1.00502751
Moles of Water (mol)	0.054942812	0.055248813	0.05577164	0.0557875
Glucose Concentration (g/L)	29.68985099	19.87715804	10.05828198	4.07248721

Table 21.A: 30, 20, 10, and 4 g/L Glucose Sample 3 Experiment 2 Adsorption Preparation input and calculated data

	30 g/L	20 g/L	10 g/L	4 g/L
Mixture Aliquot Taken Post Adsorption (mL)	0.5	0.5	0.5	0.5
Mass of Aliquot (g)	0.5029	0.4987	0.4918	0.4956
Mass of Glucose based on Original Concentration (g)	0.01464544	0.009764321	0.00487452	0.00200012
Volume of Water Added (mL)	14.5	8.8	4.55	1.56
Mass of Water Added (g)	14.4475	8.7704	4.5483	1.563
New Glucose Concentration (g/L)	0.976362666	1.049926993	0.96525152	0.97093375

Table 22.A: 30, 20, 10, and 4 g/L Glucose Sample 3 Experiment 2 Dilution Preparation input and calculated data for HPLC Analysis

	1 g/L	AC (1 g/L)	Empty (1 g/L)
Volume of Cellobiose Solution (mL)	1	1	1
Mass of Cellobiose Solution (mL)	1.0053	1.0036	1.0088
Mass of Cellobiose (g)	0.000984995	0.000983329	0.000988424
Moles of Cellobiose (mol)	5.46746E-06	5.45821E-06	5.48649E-06
Mass of Water (g)	1.004315005	1.002616671	1.007811576
Moles of Water (mol)	0.055747954	0.055653682	0.055942043
Cellobiose Concentration (g/L)	0.984995036	0.983329372	0.988424343

Table 23.A: 1 g/L, Activated Carbon, and Blank Cellobiose Sample 1 Experiment 3 Adsorption Preparation input and calculated data

	10 g/L	4 g/L
Volume of Cellobiose Solution (mL)	1	1
Mass of Cellobiose Solution (mL)	1.0098	1.0067
Mass of Cellobiose (g)	0.009908985	0.003970978
Moles of Cellobiose (mol)	5.50023E-05	2.20419E-05
Mass of Water (g)	0.999891015	1.002729022
Moles of Water (mol)	0.055502385	0.055659919
Cellobiose Concentration (g/L)	9.908985405	3.970977794

Table 24.A: 30, 20, 10, and 4 g/L Cellobiose Sample 1 Experiment 3 Adsorption Preparation input and calculated data

	10 g/L	4 g/L
Mixture Aliquot Taken Post Adsorption (mL)	0.5	0.5
Mass of Aliquot (g)	0.5057	0.4995
Mass of Cellobiose based on Original Concentration (g)	0.005012291	0.002015863
Volume of Water Added (mL)	4.55	1.56
Mass of Water Added (g)	4.5413	1.556
New Cellobiose Concentration (g/L)	0.992532928	0.978574275

Table 25.A: 30, 20, 10, and 4 g/L Cellobiose Sample 1 Experiment 3 Dilution Preparation input and calculated data for HPLC Analysis

	1 g/L	AC (1 g/L)	Empty (1 g/L)
Volume of Cellobiose Solution (mL)	1	1	1
Mass of Cellobiose Solution (mL)	1.0085	1.0071	1.0058
Mass of Cellobiose (g)	0.00098813	0.000986759	0.000985485
Moles of Cellobiose (mol)	5.48486E-06	5.47725E-06	5.47018E-06
Mass of Water (g)	1.00751187	1.006113241	1.004814515
Moles of Water (mol)	0.055925407	0.055847772	0.055775681
Cellobiose Concentration (g/L)	0.988130402	0.98675868	0.985484937

Table 26.A: 1 g/L, Activated Carbon, and Blank Cellobiose Sample 2 Experiment 3 Adsorption Preparation input and calculated data

	10 g/L	4 g/L
Volume of Cellobiose Solution (mL)	1	1
Mass of Cellobiose Solution (mL)	1.0152	1.008
Mass of Cellobiose (g)	0.009961975	0.003976106
Moles of Cellobiose (mol)	5.52964E-05	2.20704E-05
Mass of Water (g)	1.005238025	1.004023894
Moles of Water (mol)	0.05579919	0.055731795
Cellobiose Concentration (g/L)	9.961974631	3.976105708

Table 27.A: 30, 20, 10, and 4 g/L Cellobiose Sample 2 Experiment 3 Adsorption Preparation input and calculated data

	10 g/L	4 g/L
Mixture Aliquot Taken Post Adsorption (mL)	0.5	0.5
Mass of Aliquot (g)	0.4991	0.4985
Mass of Cellobiose based on Original Concentration (g)	0.004946875	0.002011827
Volume of Water Added (mL)	4.55	1.56
Mass of Water Added (g)	4.5401	1.5581
New Cellobiose Concentration (g/L)	0.979579166	0.976615167

Table 28.A: 30, 20, 10, and 4 g/L Cellobiose Sample 2 Experiment 3 Dilution Preparation input and calculated data for HPLC Analysis

	1 g/L	AC (1 g/L)	Empty (1 g/L)
Volume of Cellobiose Solution (mL)	1	1	1
Mass of Cellobiose Solution (mL)	1.0059	1.0058	1.0017
Mass of Cellobiose (g)	0.000985583	0.000985485	0.000981468
Moles of Cellobiose (mol)	5.47072E-06	5.47018E-06	5.44788E-06
Mass of Water (g)	1.004914417	1.004814515	1.000718532
Moles of Water (mol)	0.055781227	0.055775681	0.05554832
Cellobiose Concentration (g/L)	0.985582917	0.985484937	0.981467748

Table 29.A: 1 g/L, Activated Carbon, and Blank Cellobiose Sample 3 Experiment 3 Adsorption Preparation input and calculated data

	10 g/L	4 g/L
Volume of Cellobiose Solution (mL)	1	1
Mass of Cellobiose Solution (mL)	1.0123	1.0084
Mass of Cellobiose (g)	0.009933517	0.003977684
Moles of Cellobiose (mol)	5.51385E-05	2.20791E-05
Mass of Water (g)	1.002366483	1.004422316
Moles of Water (mol)	0.055639795	0.055753911
Cellobiose Concentration (g/L)	9.933517454	3.977683528

Table 30.A: 30, 20, 10, and 4 g/L Cellobiose Sample 3 Experiment 3 Adsorption Preparation input and calculated data

	10 g/L	4 g/L
Mixture Aliquot Taken Post Adsorption (mL)	0.5	0.5
Mass of Aliquot (g)	0.5011	0.4979
Mass of Cellobiose based on Original Concentration (g)	0.004966698	0.002009406
Volume of Water Added (mL)	4.55	1.56
Mass of Water Added (g)	4.5483	1.5591
New Cellobiose Concentration (g/L)	0.983504548	0.975439703

Table 31.A: 30, 20, 10, and 4 g/L Cellobiose Sample 3 Experiment 3 Dilution Preparation input and calculated data for HPLC Analysis

Sample	Glucose Area	Peak at 17.064
1-1	141484.8	
1-2	137055.1	
1-3	141174.7	358098.9
4-1	136715.8	351677.1
4-2	136085.1	529270
4-3	134825.7	90557.2
10-1	136025.3	88455
10-2	136841.9	130351.5
10-3	135545.9	27841.2
20-1	147088.9	28347.9
20-2	144998.3	45176
20-3	147777.8	16168.1
30-1	136670.9	14961
30-2	135186.3	14882.4
30-3	136749.8	10568.9
blank	141618.7	10203.3
AC-1	120425.7	9747.7
AC-2	124927.8	
AC-3	114995.9	

Table 32.A: HPLC Data for Adsorption Experiment #2

Sample	Observed Glucose Concentration g/L	Average Concentration	St.Dev	St.Dev %
1-1	0.981310276			
1-2	0.950586763	0.970352174	0.014003811	1.443167928
1-3	0.979159484			
4-1	0.948233446			
4-2	0.943859037	0.942405524	0.005449668	0.578272096
4-3	0.93512409			
10-1	0.943444276			
10-2	0.94910805	0.94422386	0.003710834	0.393003595
10-3	0.940119253			
20-1	1.020179193			
20-2	1.005679209	1.016938556	0.008197038	0.806050508
20-3	1.024957265			
30-1	0.947922028			
30-2	0.93762514	0.944672144	0.00498799	0.528012811
30-3	0.948469263			
blank	0.982238979			
AC-1	0.83524857			
AC-2	0.866474235	0.83310379	0.028163321	3.380529753
AC-3	0.797588563			

Table 33.A: Diluted Glucose Concentration Data for Adsorption Experiment #2 Based on Calibration Curve

Sample	Mass Glucose Observed	Avg. Mass Glucose Observed	St.Dev	St.Dev %
1-1	0.00098131			
1-2	0.000950587	0.000970352	1.40038E-05	1.443168
1-3	0.000979159			
4-1	0.001953361			
4-2	0.00194435	0.001941355	1.12263E-05	0.578272
4-3	0.001926356			
10-1	0.004764394			
10-2	0.004792996	0.00476833	1.87397E-05	0.393004
10-3	0.004747602			
20-1	0.009487666			
20-2	0.009352817	0.009457529	7.62325E-05	0.806051
20-3	0.009532103			
30-1	0.01421883			
30-2	0.014064377	0.014170082	7.48198E-05	0.528013
30-3	0.014227039			
blank	0.000982239	0.000982239		
AC-1	0.000835249			
AC-2	0.000866474	0.000833104	2.81633E-05	3.38053
AC-3	0.000797589			

Table 34.A: Diluted Glucose Mass Data for Adsorption Experiment #2 Based on Observed Concentration

Sample	Mass Glucose Calculated	Avg. Mass Glucose Calculated	St.Dev	St.Dev %
1-1	0.00100197			
1-2	0.001005982	0.001003038	2.11E-06	0.210101
1-3	0.001001163			
4-1	0.00202393			
4-2	0.002008599	0.002010883	9.85E-06	0.490016
4-3	0.00200012			
10-1	0.00490723			
10-2	0.004951831	0.004911194	3.17E-05	0.645185
10-3	0.00487452			
20-1	0.00982893			
20-2	0.009746699	0.009779983	3.54E-05	0.361456
20-3	0.009764321			
30-1	0.01467456			
30-2	0.014581372	0.014633791	3.89E-05	0.265997
30-3	0.01464544			
blank	0.000976131	0.000976131		
AC-1	0.001014617			
AC-2	0.001009	0.001012243	2.37E-06	0.23452
AC-3	0.001013111			

Table 35.A: Diluted Glucose Mass Data for Adsorption Experiment #2 Based on Calculated Concentration

Sample	Mass of Polymer Bead/AC	Average Mass of Polymer Bead/AC	St.Dev	St.Dev %
1-1	0.0998			
1-2	0.1003	0.1	0.000216025	0.21602469
1-3	0.0999			
4-1	0.0994			
4-2	0.1006	0.100233333	0.000590668	0.589293154
4-3	0.1007			
10-1	0.1012			
10-2	0.0994	0.099733333	0.0010873	1.090207649
10-3	0.0986			
20-1	0.1022			
20-2	0.099	0.100666667	0.001309792	1.30111806
20-3	0.1008			
30-1	0.0993			
30-2	0.0996	0.099433333	0.000124722	0.125432698
30-3	0.0994			
blank				
AC-1	0.0996			
AC-2	0.1018	0.1005	0.00094163	0.936945067
AC-3	0.1001			

Table 36.A: Polymer Bead Mass Data for Adsorption Experiment #2

Sample	Average Mass of Adsorbed Glucose	Mass of Adsorbed Glucose/Mass of Polymer Bead or AC
1 g/L	3.26862E-05	0.000326862
AC	0.000179139	0.001782476
4 g/L	6.95276E-05	0.000693658
10 g/L	0.000142863	0.001432452
20 g/L	0.000322455	0.003203193
30 g/L	0.000463709	0.004663512

Table 37.A: Polymer Bead Mass Data for Adsorption Experiment #2